LEP Note 595
Note PS/LPI/87-35 23. 9. 1987

TRANSVERSE MODE MEASUREMENTS WITH POSITRONS IN EPA

D. BRANDT, J.P. DELAHAYE, A. HOFMANN

1. Introduction

The aim of this note is to present a summary of the different machine studies dedicated to the measurement of the modes in the transverse planes and presented in section 2.

Initially, our objective was twofold: firstly, we hoped to get some precise information on the transverse impedance model, since contrarily to the previous measurements with electrons [1] any effect related to trapped ions can be excluded. Secondly we aimed at a careful study of the behaviour of the transverse dipole modes ($m = \pm 1$) in order to compare it with that predicted by the theory, and observe an eventual mode coupling which - although predicted with a threshold of $6\ 10^{10}$ particles in a single bunch - did not give rise to any instability even with a number of charges four times superior.

However, the analysis of the collected data presented in section 4 suddenly enlarged our objectives when A. Hofmann suggested that - according to the present understanding of the model reviewed in section 3 - it should be possible to derive longitudinal parameters of the machine directly from the transverse measurements. In Section 5, we present our latest estimate of the transverse and longitudinal impedances derived from the tune-shifts measurements, whereas Section 6 reflects our preliminary conclusions as well as some recommendations for future measurements.

2. Measurements

2.1 Observation of the mode m=0 (or tune)

As reviewed in section 3, the measurement of the frequency shift, $\Delta f(m)$ of the mode $m = 0$, as a function of the bunch population (N/k), is an essential ingredient for the evaluation of the effective transverse impedance Z_t, since the derivative of this function - namely $\Delta f/\Delta N$ - is directly proportional to the latter (assuming the bunch length, σ_s, is known).

However, experiments with electrons have demonstrated [1] that the measured frequency shifts were strongly dependent on both the number and the repartition of the bunches along the ring circumference. As a matter of fact, the measured shifts moved from negative values (with a single bunch) to positive ones (with 2, 4 or 8 bunches) and this effect was clearly related to the fields induced by positive ions trapped in the beam potential. As a consequence, the transverse impedances deduced from the electron behaviour were doubtful even in a single bunch where some ion perturbation could not be completely excluded.

On the contrary, the positive charge of a positron beam cleans the beam from positive ions even in the case of a multibunch operation as shown on fig. 1 which illustrates the measured tune shifts as a function of the intensity for one and eight bunches. In fact, the behaviour of both the single bunch and the multibunch beam are very similar with negative tune shifts in both cases and a slight difference in their slopes attributed to "memory" effects: the fields induced by the beam in localized impedances have not enough time to decay between two successive bunch passages leading to a slightly higher effective impedance.

During this first session, the tune shifts have been recorded for both the horizontal and vertical planes in an intensity range from 10^9 to 1.5 10^{10} particles in a single bunch (0.4 to 5.8 mA) with the corresponding results:

Horizontal : $\frac{\Delta f_x}{\Delta N}$ (m = 0) = - 6.0 10^{-8} Hz/e^+

Vertical : $\frac{\Delta f_y}{\Delta N}$ (m = 0) = - 13.6 10^{-8} Hz/e^+

which confirmed the measurements previously obtained in the vertical plane with electrons (- 11.7 10^{-8} Hz e^+) [1].

2.2 Observation of the mode m = -1

Typical pictures of the spectrum analysis of the vertical single bunch response to a frequency excitation are presented on fig. 2 with the usual operational conditions of EPA working at 500 MeV with an RF voltage of 45 kV and transverse chromaticities slightly positive. The modes have been generally investigated at their lowest frequency response (equation 3.1)

$$n = 0,\ p = -4\ f_y = (-4 + Q_y)\ f_0 + mfs = (942.34 + 4.71\ m)\ kHz$$

The mode, m = 0, is clearly visible as well as its negative shift with the intensity but no sign of higher mode appears up to 3.10^{10} particles per bunch (fig. 2 a - e). However, for a larger number of charges, because of the frequency shift of the mode m = 0, the frequency distance between modes 0 and -1 has sufficiently reduced such as to make an energy transfer between modes possible. As a consequence, the mode m = -1, shows up for charges above 4.10^{10} particles (fig. 2 f to j) with a signal response increasing with the intensity.

Indeed, as illustrated on fig. 3, the power spectrum of the hermitian modes $\pm$ 1 , maximum around 200 MHz, is negligible at the relatively low frequency ($\sim$ 1 MHz) of the tune measurement. Tentatives to observe the modes at higher harmonic frequencies failed because of a too low signal response above a frequency of 100 MHz certainly due to the limited bandwidth of the beam excitation and response measurement loop.

2.3 Observation of higher order transverse modes

As already observed on DCI [2], the presence of higher order transverse modes can be magnified at low intensity by increasing the positive chromaticity, ξ, in order to shift the mode power spectrum of the bunch to the frequency of observation by [3]

$$\Delta f_\xi = \xi \frac{Q}{\alpha_p} f_0 = Q' \frac{f_0}{\alpha_p} \qquad (Q' = \xi Q)$$

which in the case of EPA:

$f_0 = 2.38567$ MHz is the revolution frequency

$\alpha_p = 3.3\ 10^{-2}$ is the momentum compaction factor

corresponds to: $\Delta f_\xi = [\text{MHz}] = 72.293\ Q'$

Indeed, with a vertical chromaticity, Q' = 2, shifting the mode power spectrum (fig. 3) by 145 MHz, the modes m = $\pm$ 1 become visible over the whole intensity range extending up to the charge of $2.8\ 10^{11}$ particles in a single bunch (fig. 4).

Again by energy exchange, the mode, m = -2, is magnified for charges above 2.10^{10} particles (fig. 4c), as well as the modes m = -3 and -4 for charges above 9.10^{10} (fig. 4g) and $12.5\ 10^{10}$ particles (fig. 4i) respectively.

Observation of higher transverse modes up to + 3 and - 4 from vanishing currents is possible by raising the chromaticity Q'_y to + 4 (fig. 5) but according to the impedance model (fig. 3) deduced from equipment measurements [1], the power spectrum of the modes, shifted by as much as 290 MHz interacts with a reduced imaginary part of the impedance therefore affecting the corresponding effective impedance $Z^0_{y\ eff}$.

The general behaviour of the modes is globally illustrated on figs. 4 and 5 where both the shift and coupling of the modes are clearly visible. An especially interesting case is observed on fig. 5 e, where for $N = 3.10^{10}$ particles in a single bunch, the signal response of the m = -1 mode suddenly becomes larger than that of the m = 0 mode. Although no sign of vertical instability shows up, the modes 0 and -1 for larger numbers of charges, cannot be distinguished one from the other as their respective frequencies merge together (figs. 4 f to l and 5 f to j). Actually this phenomenon of energy exchange between modes, also observed in simulations, is usually considered as the signature for the onset of the mode coupling.

In fact, their real frequency spread of ~ 1 kHz is artificially enlarged by a measurement averaging necessary to cope with a tune jitter of initially up to $\pm$ 2.5 10^{-3} (case of figs. 2 and 5). This jitter could be reduced by about a factor three (case of fig. 4) after adoption for the whole LPI complex powering of the more stable network derived from the SPS and the fine tuning of the lattice quadrupole power supply regulation [3].

2.4 Modes observation with a different RF voltage

In order to check the model described in section 3, the modes behaviour has been observed with an RF voltage on the cavity gap reduced from 45 to 20 kV. Clean signals and data could be collected at low intensity but the identification of the modes became impossible for charges above 3.10^{10} particles (fig. 6).

3. Mode shift behaviour

The frequency shift Δf (m) for the mode m of a bunch with a charge, N/k, and a length, σ_s, interacting with an effective transverse impedance $Z^m_{t\ eff}$ is usually given by [4]:

$$\Delta f\ (m) \alpha \frac{f_0}{|m|+1} \frac{Z^m_{t\ eff}}{\sigma_s} \frac{N}{k}$$

which suggests that:

- the behaviour of the modes $\pm$ 1 should be identical
- for the same current, their shift should be half of that of the mode m = 0.

However, when considering the fig. 7 representing the shifts of the observed modes with the charge per bunch in a first series of measurements (test 3 of section 4), these two statements are obviously not verified.

The key to the explanation came from M.P. Level who participated in the same kind of measurements on DCI [2] and pointed out the influence of the variation of the synchrotron frequency f_s due to the potential well induced by the interaction of the bunch with the longitudinal ring impedance (Z_L/r).

Indeed, the frequencies of the possible transverse modes, m, are given by [4]:

$$f_{p,m,n} = (n + pk + Q_{x,y})\, f_0 + m\, f_s \qquad (3.1)$$

where f_0 = 2.38567 MHz is the revolution frequency

k is the number of bunches

n and p are both integer numbers such that:

$0 < n < k - 1 \qquad -\infty < p < +\infty$

$Q_{xo,yo}$ = 4.554, 4.395 are the horizontal, vertical tunes at vanishing current

$Q_{x,y}(m)$ are the real tunes affected by the interaction of the beam with the imaginary part of the transverse effective impedance $Z^m_{t\ eff}$ [5]:

$$Q_{x,y} = Q_{xo,yo} - \frac{jec}{4\pi}\ \frac{\beta_{x,y}}{|m|+1}\ \frac{e}{E}\ \frac{Z^m_{t\ eff}}{\tau_L}\ \frac{N}{k} \qquad (3.2)$$

$\beta_{x,y}$ are the β functions at the impedance location

E is the operating energy

N is the total number of particles

τ_L is the overall bunch length depending on the particle distribution. In case of a gaussian distribution with a standard deviation σ_s [5,6] $\tau_L \sim 4\ \sigma_s$

f_s is the synchrotron frequency modified by the potential well which becomes below the longitudinal turbulence threshold [5.6]:

$$f_s^2 = f_{so}^2 \left[1 - 12\, jec \frac{R^2}{\tau_L^3} \frac{1}{hV|\cos\varphi|} \left| \frac{Z_L}{r} \right| \frac{N}{k} \right] \tag{3.3}$$

Introducing the synchrotron frequency at vanishing current:

$$f_{so} = \frac{c}{2\pi \sqrt{2\pi}} \frac{\alpha_p^{1/2}}{R} \left[\frac{e}{E} \right]^{1/2} (hV\,|\cos\varphi|)^{1/2} \tag{3.4}$$

the linear dependence of the synchrotron frequency for low current becomes

$$f_s \sim f_{so} - \frac{3je\,c^2}{2\pi \sqrt{2\pi}} \left[\frac{\alpha_p\, e}{E} \right]^{1/2} \frac{R}{\tau_L^3} \frac{1}{(hV|\cos\varphi|)^{1/2}} \left(\frac{Z_L}{r}\right) \frac{N}{k} \tag{3.5}$$

where $\alpha_p = 3.3\ 10^{-2}$ is the momentum compaction factor

$R = 20$ m is the ring mean radius

h, V are the RF harmonic number and voltage on the cavity gap

Therefore at low current and below the longitudinal turbulence threshold, the frequency shift $\Delta f(m)$ with the charge per bunch N/k of the mode m becomes:

$$\Delta f(m) = \underbrace{\Delta f_t^m}_{\substack{\text{contribution of the} \\ \text{transverse impedance}}} + \underbrace{\Delta f_L^m}_{\substack{\text{contribution of the} \\ \text{longitudinal impedance}}} \tag{3.6}$$

where:

$$\Delta f_t^m = f_0\, \Delta Q_{x,y}(m) = -\frac{3.82\ 10^{-12}}{|m|+1} jf_0\, \beta_{x,y} \frac{Z_{t\,eff}^m}{\tau_L} \frac{e}{E} \Delta\left[\frac{N}{k}\right] \tag{3.7}$$

$$\Delta f_L^m = m\, \Delta fs = -5.48\ 10^{-3}\, mj \left(\frac{\alpha_p e}{E}\right)^{1/2} \frac{R}{\tau_L^3 (hV|\cos\varphi|)^{1/2}} \left|\frac{Z_L}{r}\right| \Delta\left[\frac{N}{k}\right] \tag{3.8}$$

As a consequence, the shifts of the modes + 1 and - 1 are different one from the other and not equal to half of the zero mode. Moreover, the separated contributions from the longitudinal and the transverse impedances can be easily extracted, assuming an equivalent effective impedance for the modes $\pm$ 1:

$$\Delta f \ (m = 0) = \Delta f_t^0 \qquad (3.9)$$

$$\Delta f \ (m = +1) = \Delta f_t^1 + \Delta f_L^1 \qquad (3.10)$$

$$\Delta f \ (m = -1) = \Delta f_t^1 - \Delta f_L^1 \qquad (3.11)$$

$$\Rightarrow \quad \Delta f_t^1 = \frac{1}{2}\left[\Delta f \ (m = +1) + \Delta f \ (m = -1)\right]$$

$$\Delta f_L^1 = \frac{1}{2}\left[\Delta f \ (m = +1) - \Delta f \ (m = -1)\right]$$

These relations can be very useful to determine the effective transverse impedance for modes 0 and ± 1 but also to deduce from purely transverse measurements fundamental longitudinal parameters like the longitudinal impedance, as well as the incoherent synchrotron frequency:

$$f_s^{inc}(N/k) = f_{so} + \Delta f_s^{inc}(N/k) = f_{so} + \Delta f_L^1(N/k) \qquad (3.12)$$

4. Measurement analysis

In fact, five series of measurements have been performed with various values of RF voltages, vertical chromaticities and intensities.

The relevant parameters of these tests are listed in the table 1 (Appendix) while figs. 7, 8, 9 and 10 illustrate the measured frequencies of the corresponding modes as a function of the charge per bunch.

4.1 Comparison with simulations

In order to compare these results with simulations, T. Suzuki (on leave from KEK in the LEP-TH group) performed a few MOSES runs [7] taking into account both the experimentally measured bunch length [8] at each current and the transverse effective impedance deduced from beam measurements in section 5.

The calculated real shifts of the modes m = 0 and ± 1 in the case of a vertical chromaticity, $Q'_y = +2$ and a RF voltage on the cavity gap, V = 45 kV, are illustrated on figs. 8 and 9 together with the corresponding beam measurements for a better comparison.

The modes m = 0, -1, -2 and -3 show a fair agreement between measurements and simulation along the whole intensity range. On the other hand, the measured shift of the mode m = +1 is significantly different from the simulation which remains unexplained.

A coupling of the modes m = 0 and m = -1 is observed without any sign of instability above a threshold of 6.10^{10} particles as expected from simulation. The absence of instability is also in agreement with the simulation which shows that the growth time of the instability deduced from the imaginary part of the mode frequency shift is always smaller than the damping time constant provided by the head tail damping. This result has always been observed with long bunches as in this case, the real part of the effective impedance which drives the instability is small in the low frequency range of modes 0 and -1 spectra (fig. 3).

At higher currents, the two modes merge in a single one and cannot be differentiated one from the other up to a charge of $2.8\ 10^{11}$ particles in a single bunch (figs. 4 and 9) representing more than 4.5 times the mode coupling threshold.

Because of the coupling between the modes 0 and -1 the next mode coupling does not involve the modes 0 and -2 but the modes -2 and -3 with a threshold of $2.0\ 10^{11}$ particles in a single bunch (figs. 4 and 9).

4.2 Comparison with the analytical calculation

In order to test the analytical model of Section 3, the dependence of the transverse and longitudinal contributions to the shift of the modes 0 and $\pm$ 1 - as measured in the typical case of test 2 (Q'_y = +2 and V_{RF} = 45 kV) - are plotted on figs. 11, 12 and 13 as a function of appropriate scaling parameters, which take into account the measured bunch length σ_s at the corresponding beam current [8].

Indeed, as suggested by the analytical model, the measured frequency shift of the mode m = 0 as well as the one simulated by MOSES in the same conditions are very linear as a function of the parameter $N/(k\ \sigma_s)$ up to a charge around 6.10^{10} e^+ where the frequency of the mode m = 0 is perturbed by the coupling with the mode m = -1 (fig. 11). The slope of this function is strictly proportional to the effective transverse impedance and will be used in section 5 to evaluate it.

This is also true for the transverse impedance of the modes m = $\pm$ 1 as illustrated on fig. 12. Assuming, in the case of long bunches, equivalent effective impedances for modes 0 and $\pm$ 1 (fig. 3), the ratio of the respective transverse contribution of the mode m = 0 to the one of the mode m = $\pm$1 should be equal to:

$$\frac{\Delta f_t^1}{\Delta f_t^0} = \frac{1}{|m|+1} = 0.5$$

In fact, B. Zotter pointed out that this coefficient had been derived for a parabolic particle distribution, and should rather be:

$$\frac{1}{(|m|+1)^{1/2}} = 0.7$$

in the case of the gaussian particle distribution of an electron bunch [9]. This is particularly well confirmed by the measurements (figs. 11,12):

$$\frac{\Delta f_t^1}{\Delta f_t^0} = \frac{6.4 \times 10^{-12}}{9.15 \times 10^{-12}} = 0.699$$

On the other hand, simulation with MOSES yields a very different ratio:

$$\frac{\Delta f_t^1}{\Delta f_t^0} = \frac{2.73 \times 10^{-12}}{10.7 \times 10^{-12}} = 0.255 \quad !$$

which is clearly related to the fact that MOSES did not reproduce correctly the behaviour of the mode m = +1.

The longitudinal dependence of the shift of the modes m = $\pm$ 1 deduced from the difference of the measured shifts of the mode m = + 1 and of the mode m = -1 is in agreement with the analytical formulation (3.8). It is linear as a function of the parameter $N/(k\sigma_s)$ as shown on fig. 13 for low intensities.

For charges above 2.10^{10} particles, corresponding to the longitudinal turbulence threshold [8], the dependence is also linear but with a sudden change of slope. At the threshold of the mode coupling (around 6.10^{10} e^+) where the shift of the mode m = -1 becomes affected by the coupling with the mode m = 0, the behaviour becomes completely chaotic.

The variation of this function is particularly interesting as it provides a direct measurement of the relative reduction of the incoherent synchrotron frequency by potential well. The slope of this function at low current is proportional to the longitudinal effective impedance and will be used in section 5 to estimate it.

Finally, the transverse and longitudinal contributions to the shift of the modes 0 and $\pm$ 1 are summarized in the table 1 in the Appendix for the different series of measurements after a linear fit of the measured mode frequencies at low current up to 1.5 10^{10} particles per bunch below the longitudinal turbulence threshold [8].

It is worth noting, that the shift of the mode 0 in each of these five tests is significantly higher than the value (13.10^{-8} Hz/e$\pm$) obtained both with electrons [1] and in the explorating measurements with positrons described in section 2. In fact, in both cases, this value had been obtained from a linear fit of measurements covering a large intensity range extending over the longitudinal turbulence threshold and was therefore affected by a strong bunch lengthening [8].

5. Transverse and longitudinal impedances

5.1 Transverse impedance

According to the model valid at low current and below the longitudinal turbulence, the transverse effective impedance $Z_{t\ eff}^{m}$ weighted by the local $\beta_{x,y}$ function at the impedance location can be deduced from the transverse contribution of the frequency shift with current for any mode, m, assuming the effective impedance for the modes $\pm$ m are equivalent. In the case where the ring impedance can be assimilated to the one of a broad band resonator, this assumption is strictly valid only for a zero chromaticity. Nevertheless for long bunches, it is always true as long as the power spectrum of the mode m remains within the low frequency range of the resonator where the imaginary part of the impedance is nearly constant.

Assuming a total bunch length $\tau_L = 4\ \sigma_s$, in the case of a gaussian distribution [5, 6], one has:

$$Z_{t\ eff}^{m} = - \left[\frac{|m| + 1}{9.55\ 10^{-13}} \frac{\sigma_s}{f_0\ \beta_{x,y}} \left(\frac{E}{e}\right) \right] \underbrace{\frac{1}{2} \left[\frac{\Delta f(+m) + \Delta f(-m)}{\Delta (N/k)} \right]}_{\Delta f_t^m} \qquad (5.1)$$

This formulation simplifies for the mode zero as there is no longitudinal contribution to the shift of this particular mode with the charge per bunch.

$$Z_{t\ eff}^{0} = - \frac{\sigma_s}{9.55\ 10^{-13}\ f_0\ \beta_{x,y}} \left(\frac{E}{e}\right) \frac{\Delta f\ (m=0)}{\Delta\ (N/k)} \qquad (5.2)$$

In the case of EPA working at 500 MeV with an impedance localised in the kicker modules (β_x = 13.6 m, β_y = 3.5 m) as derived from systematic impedance measurements of all the elements implemented in the ring, the horizontal and vertical impedances become [1]:

$$Z^0_{x\ eff} = - \frac{\sigma_s}{6.2\ 10^{-14}} \quad \frac{\Delta f_x\ (m = 0)}{\Delta\ (N/k)} \tag{5.3}$$

$$Z^0_{y\ eff} = - \frac{\sigma_s}{1.6\ 10^{-14}} \quad \frac{\Delta f_y\ (m = 0)}{\Delta\ (N/k)} \tag{5.4}$$

A first approximation of the effective vertical impedance for the mode m = 0 can be obtained from a linear fit of the measurements at low current ($< 1.5\ 10^{10}\ e^+$) below the turbulence threshold (table 1). A better estimation is derived from the fig. 11 linearising the mode m = 0 frequency shift by an appropriate choice of the abscissa parameter

$$\frac{\Delta f_y\ (m=0)}{f_{so}} = \left[\frac{\Delta Q_y}{Q_{so}}\right]_{measured} = - 9.15\ 10^{-12}\ \frac{N}{k\ \sigma_s}$$

which, using equation (5.4) with a synchrotron frequency, f_{so} = 4.71 kHz yields:

$$Z^0_{y\ eff} = \frac{9.15\ \ 10^{-12}\ x\ 4.71\ 10^3}{1.6\ \ 10^{-14}} = 2.7\ M\Omega/m$$

thus not far from the impedance model ($Z^0_{y\ eff}$ = 2.9 MΩ/m).

A MOSES calculation, plotted on the same graph (fig. 11), demonstrates also a very linear dependence of the mode (m = 0) frequency shift as a function of the parameter $N/(k\ \sigma_s)$ up to the mode coupling threshold:

$$\frac{\Delta f_y\ (m = 0)}{f_{so}} = \left[\frac{\Delta Q_y}{Q_{so}}\right]_{Moses} = - 10.7\ 10^{-12}\ \frac{N}{k\ \sigma_s}$$

The measured data would therefore be best fitted by a MOSES calculation based on a corrected effective impedance (fig. 11)

$$Z^0_{y\ eff} = \frac{9.15\ 10^{-12}}{10.7\ 10^{-12}} x\ 2.9 = 2.5\ M\Omega/m$$

In fact, the analytical formulation (eq. 3.7) and the MOSES calculation based on the same parameters yield 8% different shifts of the mode m=0. Their prediction would be similar if the relation between the total bunch length, τ_L, and its standard deviation σ_s would be corrected to:

$$\tau_L = 3.7\ \sigma_s$$

instead of the $\tau_L = 4\ \sigma_s$ used.

The test 5 (Table 1) with a somewhat different bunch length yields a 10% higher effective impedance ($Z^0_{y\ eff} = 3\ M\Omega/m$) confirming that the bunch length is not exactly taken into account by the analytical model.

5.2 Longitudinal impedance

From these purely transverse measurements, the longitudinal impedance can be deduced from the longitudinal contribution of the shifts of the modes ± 1 and compared with the estimation [8] obtained from bunch length measurements. Again, assuming a total bunch length, $\tau_L = 4\ \sigma_s$, in the case of a gaussian distribution [5,6]:

$$\left(\frac{Z_L}{r}\right) = \frac{\sigma_s^3\ (hV|\cos\varphi|)^{1/2}}{8.56\ 10^{-5}\ R} \left[\frac{E}{e\ \alpha_p}\right]^{1/2} \underbrace{\frac{1}{2}\ [\Delta f\ (m=+1) - \Delta f\ (m=-1)]}_{\Delta f_L^1} \quad (5.5)$$

which in the case of EPA working at 500 MeV becomes:

$$\left(\frac{Z}{r}\right) = 2.03\ 10^8\ (V\ |\cos\phi|)^{1/2}\ \sigma_s^3\ \Delta f_L^1$$

As can be seen from it, this solution is strongly dependent on the bunch length, namely to its third power. Therefore the longitudinal impedance has been deduced from the slope (at low current) of the difference of the frequency shifts between the modes m = +1 and -1 as a function of the linearising parameter $N/[k\ \sigma_s^3\ (V|\cos\varphi|)^{1/2}]$.

The case of test 2 illustrated on fig. 13 ($V_{RF} = 45$ kV, $f_{so} = 4.71$ kHz)

$$\frac{\Delta f\ (m+1) \quad \Delta f\ (m-1)}{2\ f_{so}} = 1.55\ 10^{-13}\ \frac{N}{k\ \sigma_s^3}$$

yields a longitudinal impedance:

$$\left[\frac{Z_L}{r}\right] = 2.03\ 10^8\ (4.5\ 10^3)^{1/2}\ \text{x}\ 4.71\ 10^3\ \text{x}\ 1.55\ 10^{-13} = 31.5\ \Omega$$

or 50% higher than the impedance deduced from bunch length measurements [8]

$$\left[\frac{Z_L}{r} = 21.0\ \Omega\right].$$

All the different tests including the one performed with a different RF voltage and bunch length led to similar longitudinal impedances (see table 1). In fact, because of the strong dependence of the calculated impedance to the third power of the bunch length, this result is clearly dependent on the relation between the total bunch length, τ_L, and its standard deviation σ_s.

Actually the present formulations are steadily based on approximations derived from parabolic bunch population distribution which seems to overestimate the bunch length and therefore the impedance. A. Hofmann is presently deriving the whole set of equations adapted to the gaussian distribution of an electron beam and governing the real beam induced voltage, charge distribution, bunch length and average synchrotron frequency. As soon as available, they will be applied to the present measurement or to more accurate data taken in the low intensity range.

However, it is very interesting to note that this new set of equations clearly demonstrates that - in the case of a gaussian distribution - the relevant total bunch length τ_L should be accounted for:

$$\tau_L \simeq 3.5\ \sigma_s$$

instead of the $\tau_L = 4.0\ \sigma_s$ used so far in our analytical approach.

Including this correction in our numerical evaluation yields:

$$Z^0_{t\ eff} = 2.4\ M\Omega/m$$
$$Z_{L/r} = 21.1\ \Omega$$

which should be considered as our final results.

5.3 Incoherent synchrotron frequency

As already pointed out, the variation with current of the incoherent synchrotron frequency can be directly deduced from the variation of the longitudinal contribution to the transverse mode shift (eq. 3.12):

$$\Delta f_s^{inc}/\Delta\ (N/k) = \Delta f_L^1\ /\Delta\ (N/k)$$

This variation is compared on Fig. 13 with the measured variation of the frequency of the second synchrotron side band around the 20th harmonic of the RF frequency (Fig. 14):

$$\frac{\Delta f_{s2}}{2} = -4.5\ 10^{-14}\ \Delta\left[\frac{N}{k\ \sigma_s^3}\right]$$

This gives an experimental relation between the variations with current of the effective incoherent synchrotron frequency and that of the second synchrotron side band:

$$\frac{\Delta f_{s2}\ /\ 2}{\Delta f_s^{inc}} = 0.29\ .$$

6. Conclusions

The observation of the behaviour of the transverse modes as a function of the beam intensity was carried out for different values of both the chromaticity and RF-voltage in a large intensity range. All the measurements were performed with positrons in order to confirm/explain observations made with electrons.

The main objectives achieved during these measurement sessions can be summarized as follows:

i) Fitting the detuning of the vertical mode m=0 at low intensities yields a transverse impedance of $Z_{y\ eff}^{0}$ = 2.4 MΩ/m, slightly lower than the impedance model (2.9 MΩ/m).

ii) Measurements with 8 bunches confirmed that previous measurements with electrons were affected by the presence of trapped ions. With positrons, there is an indication that the transverse tune shift might be slightly increased by multi-bunches 'memory' effects.

iii) With zero chromaticity in the machine, the transverse higher modes can only be observed above the threshold of longitudinal turbulence, making therefore the interpretation of their behaviour relatively difficult. However, by making the chromaticity slightly positive, it is then possible to observe the modes up to m = $\pm$ 3.

iv) Having recognized (with the help of M.P. Level) that the detuning of the modes m= $\pm$ 1 was composed of both a part due to the transverse impedance and a part related to the variation of the incoherent synchrotron frequency, it was possible to calculate both contributions separately. The latter procedure is potentially interesting since it allows to measure longitudinal parameters (usually difficult to measure longitudinally) directly from transverse measurements.

v) The measured real shifts of the modes 0, -1, -2 and -3 agree reasonably well with simulation and analytical models. On the other hand, the measured shifts of the mode m = +1 is significantly different from simulation with MOSES.

vi) The coupling of the modes 0 and -1 is foreseen and observed for a charge of 6.0 10^{10} particles per bunch without any sign of instability. Contrarily to previous expectations by simulation, for charges above the mode coupling threshold, the two modes having merged in a single one, remain coupled with a common frequency up to the highest charge available of 2.8 10^{11} particles in a single bunch representing more than 4.5 times the mode coupling instability threshold.

vii) For higher intensities, the next mode coupling does not involve the modes 0 and -2 as the frequency shift of the mode 0 is modified by its coupling with the mode -1, but the modes -2 and -3, again without instability and a threshold of 2.0 10^{11} particles in a single bunch.

viii) The absence of any instability at the coupling of both the modes (0, - 1) and (-2, -3) is perfectly predicted by MOSES (the imaginary part of the mode frequency shift remains negative) provided the measured bunch length is included in the calculation. In fact, thanks to the long EPA bunch length, the spectra of the low order hermitian modes extend in a low frequency range where the real part of the impedance - which drives the instability - is small. As a consequence, the growth of the instability is damped by both head tail and synchrotron radiation damping.

Finally, accurate measurements of the mode shifts would be largely improved by an increase of the bandwidth of the beam excitation - mode measurement loop - which would enable an observation at higher frequencies thus avoiding a chromaticity modification affecting the effective impedance. Moreover, a better stability of the ring power supplies would avoid the averaging of the measurements which artificially enlarges the mode spread and hides the behaviour of the individual modes in the mode coupling vicinity.

ACKNOWLEDGEMENTS

We would like to thank B. Zotter for many interesting and fruitful discussions, M.P. Level for pointing out the correct behaviour of the transverse dipole modes and to T. Suzuki for performing the numerical evaluations with MOSES.

REFERENCES

[1] J.P. Delahaye, L. Rivkin: EPA Impedance Model and Transverse Mode Measurements; PS/LPI Note 87-14

[2] M.P. Level et al.: Transverse Mode Coupling Experiment in DCI: LAL/RT/84-09

[3] G. Coudert, B. Godenzi: private communication.

[4 F.J. Sacherer: Proc. of the 9th Int. Conf. on High Energy Accelerators (1974) p. 347

[5] A. Hofmann and J. R. Maidment: Current Dependent Phenomena in LEP, LEP Note 168.

[6] J.L. Laclare: Bunched beam coherent instabilities; CERN 87-03

[7] Y.H. Chin: MOSES Users Guide, CERN/SPS/86-02 (1986)

[8] S. Bartalucci, J.F. Bottollier, K. Hübner: Note to appear on EPA bunch lengths measured with positrons. Similar measurements with electrons can be found in PS/LPI Note 87-05

[9] B. Zotter, personal communication

APPENDIX

		Test (1)	Test (2)	Test (3)	Test (4)	Test (5)
RF Voltage, V_{RF}	(kV)	45	45	45	45	20
Hor. chromaticity, Q'_x	-	0.1	0.1	0.1	0.1	0.1
Vert. chromaticity, Q'_y	-	0.1	2.0	2.5	4.0	2.0
Δf_ξ	(MHz)	7.2	145	180	289	145
Synchrotron frequency, f_s	(kHz)	4.71	4.71	4.71	4.71	3.12
Bunch length, σ_s (for $\frac{N}{k} = 10^{10}$ e^+)	(m)	0.23	0.23	0.23	0.23	0.32
Corresponding figures		2	4,9	7	5,8,9 10,11, 12,13	7
Mode zero shift at low intensity $< 1.5\ 10^{10}$ e^+: $\frac{\Delta f\ (m=0)}{\Delta N} = \Delta f^0_t/\Delta N$	(10^{-8} Hz/e^+)	- 18.1	- 19.0	- 17.6	- 24.9	- 15.0
Transverse contribution to the modes $\pm$ 1 shift $\Delta f^1_t/\Delta N$	(10^{-8} Hz/e^+)	-	- 9.7	- 7.0	- 15.4	- 10.9
Ratio $\Delta f^1_t/\Delta f^0_t$		-	0.5	0.39	0.62	0.73
Longitudinal contribution to the modes $\pm$ 1 shift: $\Delta f^1_L/\Delta N$	(10^{-8} Hz/e^+)	-	- 5.7	- 5.2	- 7.1	- 2.6
Calculated effective vertical Impedance, Z^0_{eff}	(MΩ/m)	2.62	2.73	2.53	3.58	3.00
Calculated longitudinal impedance, Z/r	(Ω)	-	29.9	27.3	37.2	24.5

Table 1: Relevant machine parameters, transverse and longitudinal contributions to the shift of the modes m = 0, $\pm$ 1 and corresponding impedances in the five series of measurements

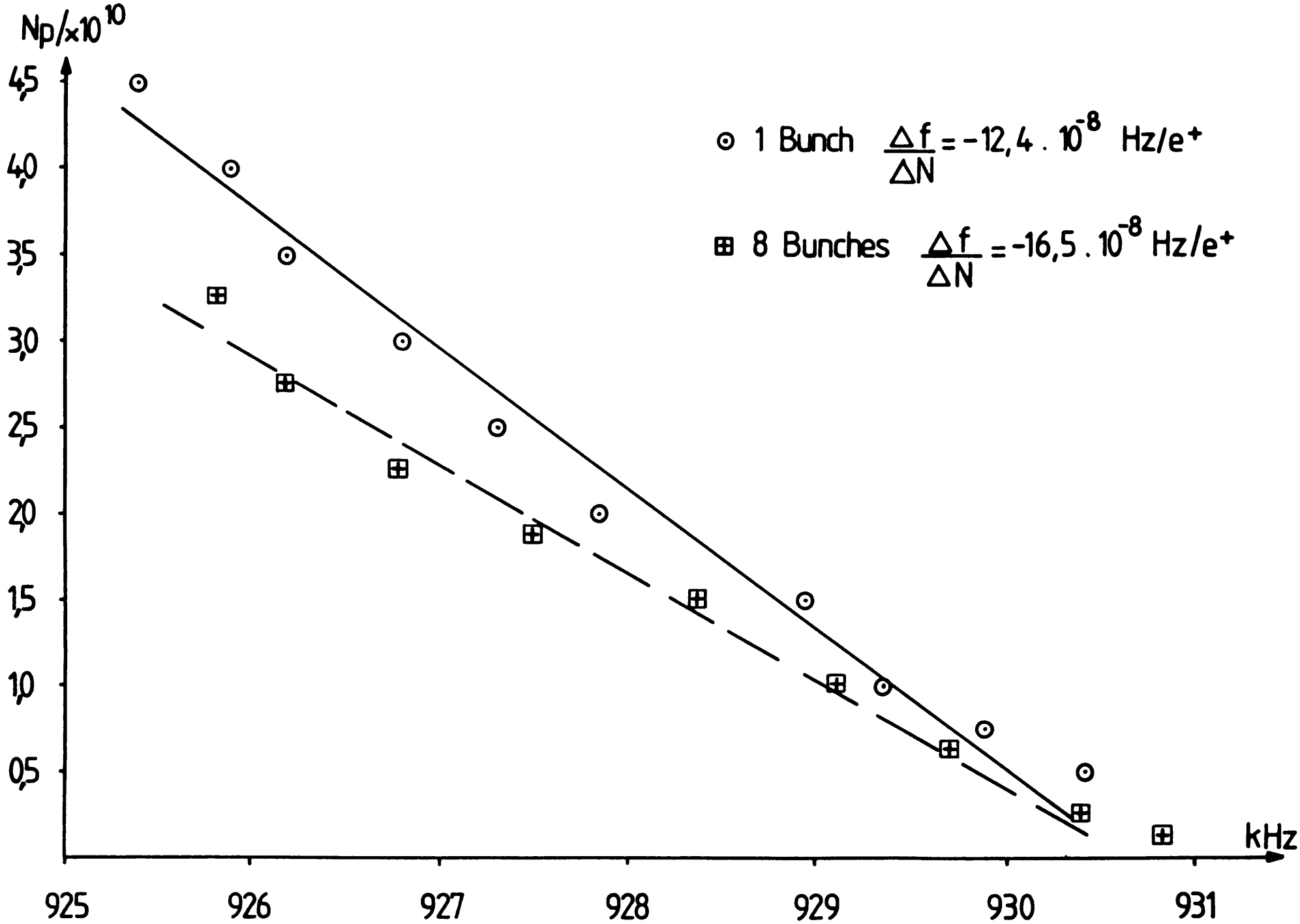

fig 1: Frequency shift of the vertical mode, m=0, with a single bunch or multibunch e^+ beam.

- fig 2 - a)

Position Single bunch Vertical mode (July 87)

E = 500 MeV $Q'_y = +0.1$ $Q'_x = +0.1$ $V_{RF} = 15$ kV $F_s = 4.71$ kHz

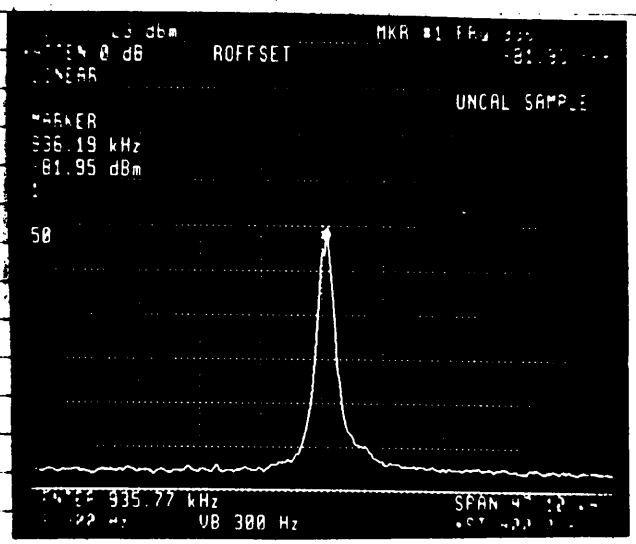

(a) N = 1.5×10^9

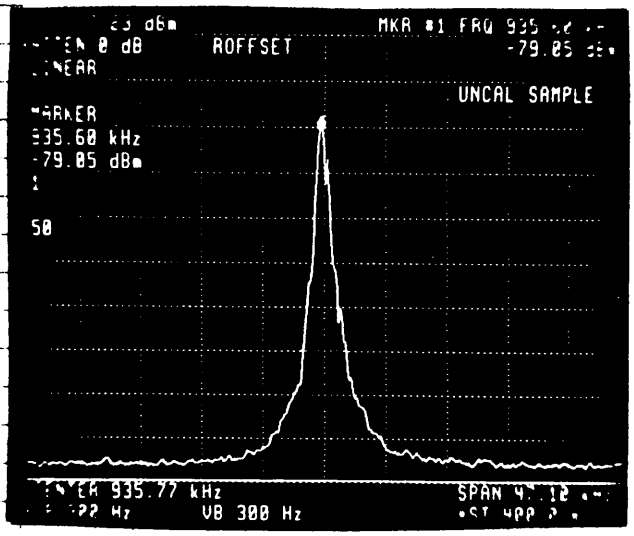

N = 5×10^9 (b)

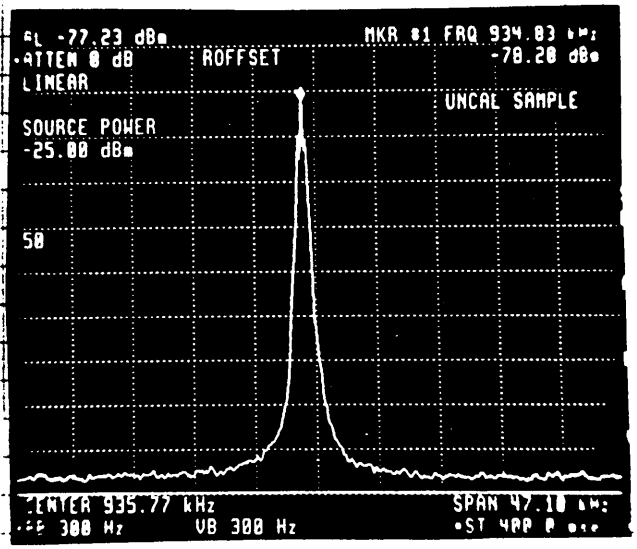

(c) N = $1. \times 10^{10}$

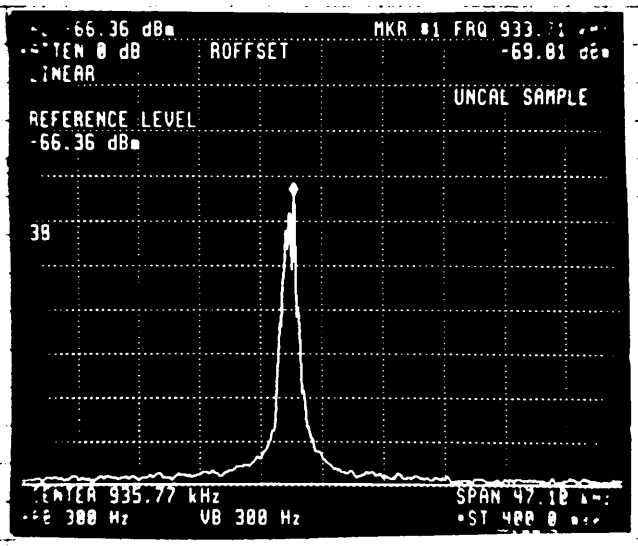

N = 2×10^{10} (d)

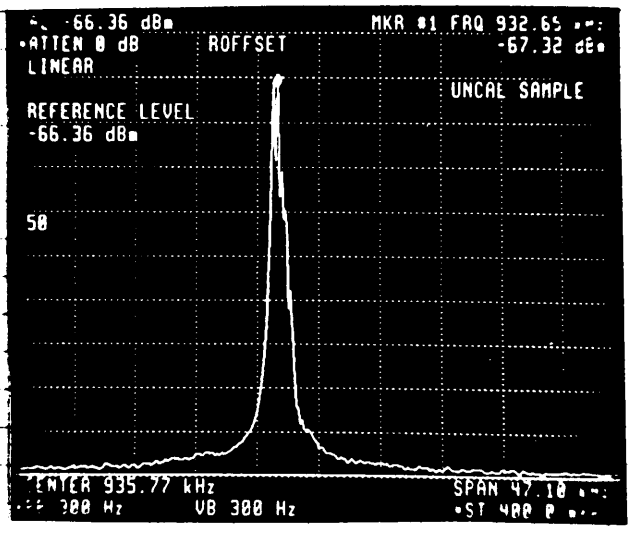

(e) N = 3×10^{10}

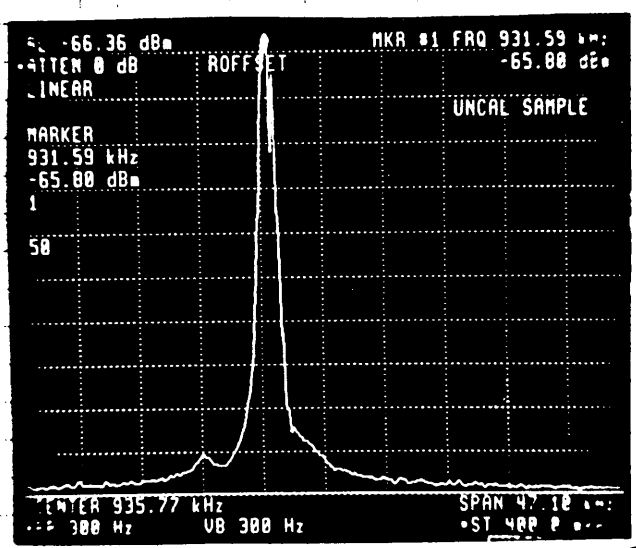

N = 4×10^{10} (f)

- fig 2 - b)

Position Single Bunch Vertical Mode (July 87)

$E = 500$ MeV $Q'_y = +0.1$ $Q'_x = +0.1$ $V_{RF} = 4.5$ kV $F_s = 4.71$ kHz

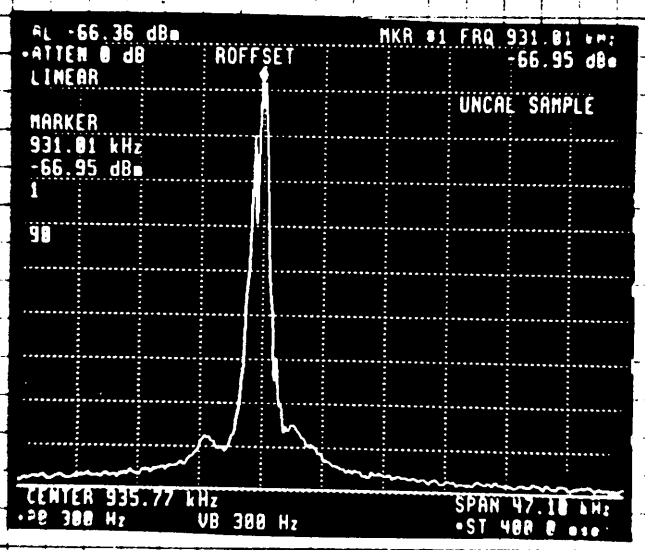

g) $N = 5 \times 10^{10}$

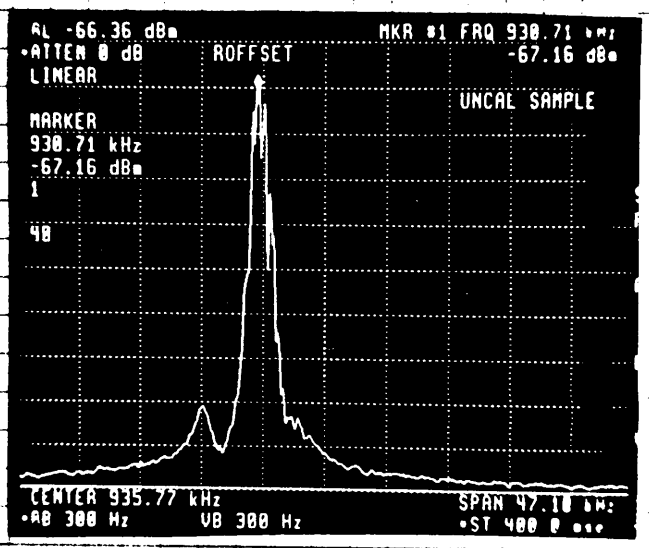

h) $N = 6 \times 10^{10}$

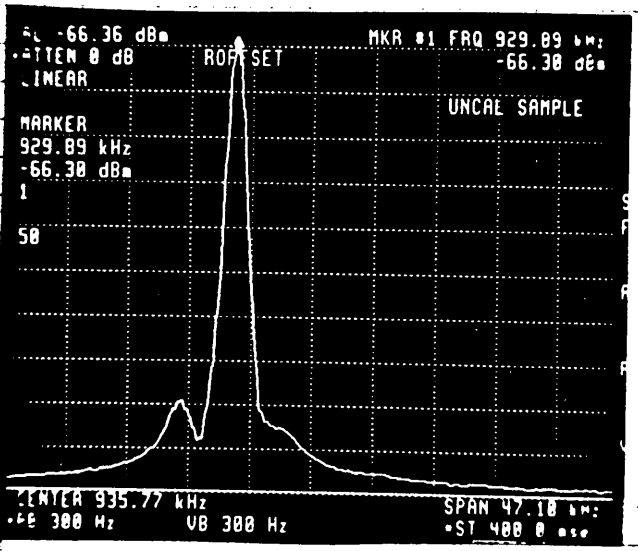

i) $N = 7 \times 10^{10}$

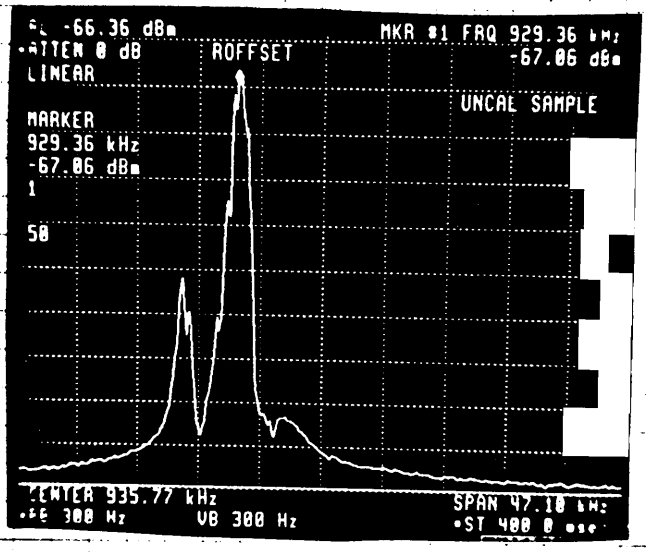

j) $N = 7 \times 10^{10}$

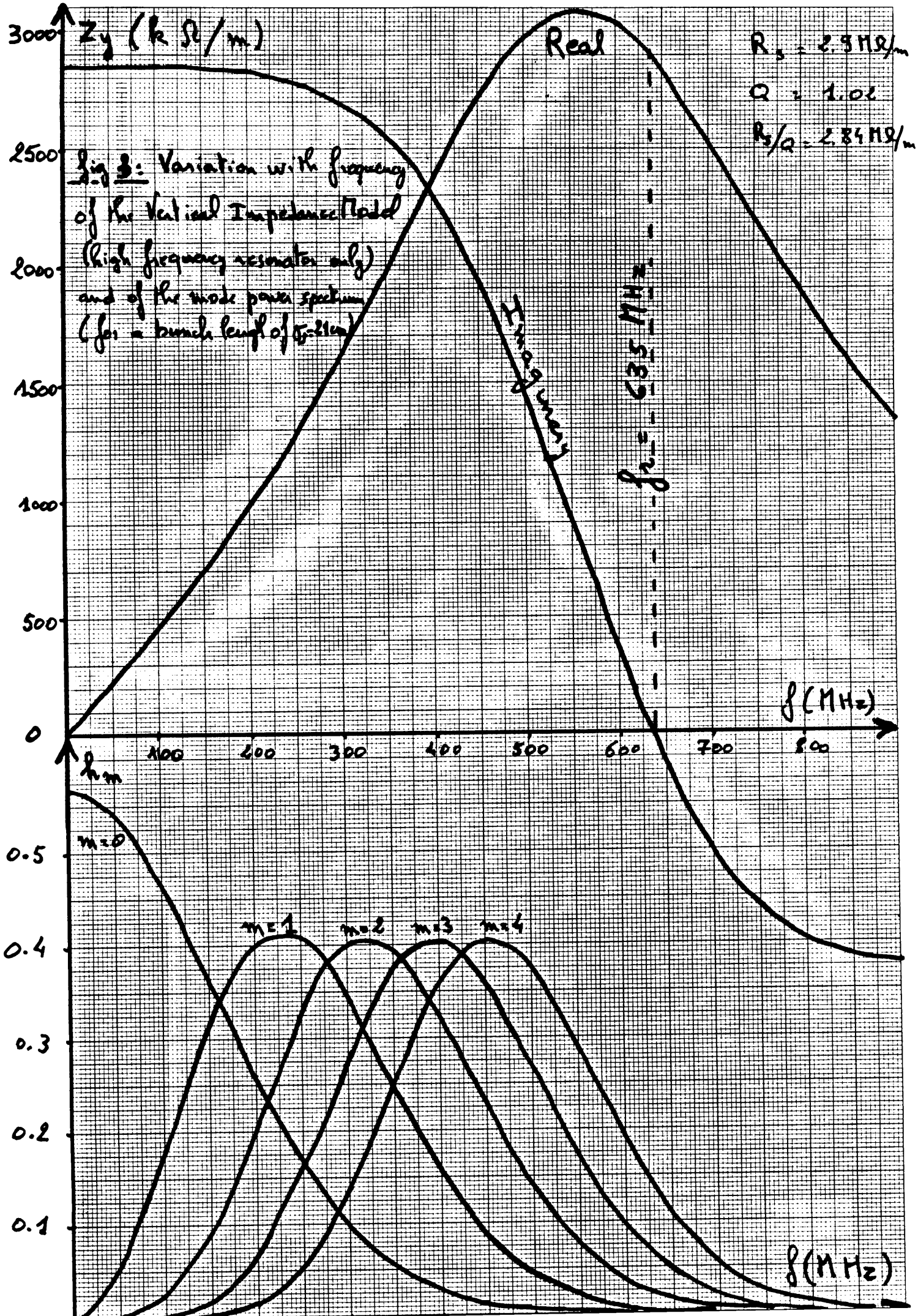

Fig 3: Variation with frequency of the Real and Imaginary Impedance (Model (high frequency resonator only) and of the mode power spectrum (h_m = bunch length of σ_z=21cm)

POSITRON SINGLE BUNCH VERTICAL MODE

fig 4 $E = 500$ MeV $\quad Q'_y = +2.0$ $\quad V_{RF} = 45$ kV

$f_{yo} = 896$ kHz $\quad Q'_x = +0.1$ $\quad F_{so} = 4.71$ kHz

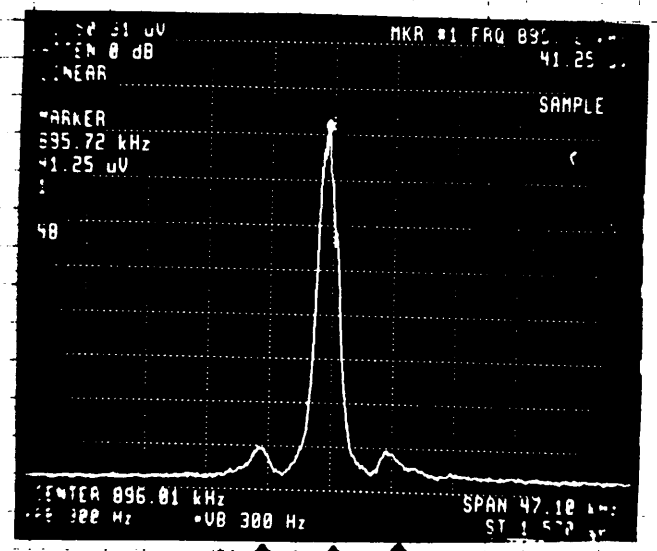

-1 0 +1

$2.2\ 10^9\ e^+$

(a)

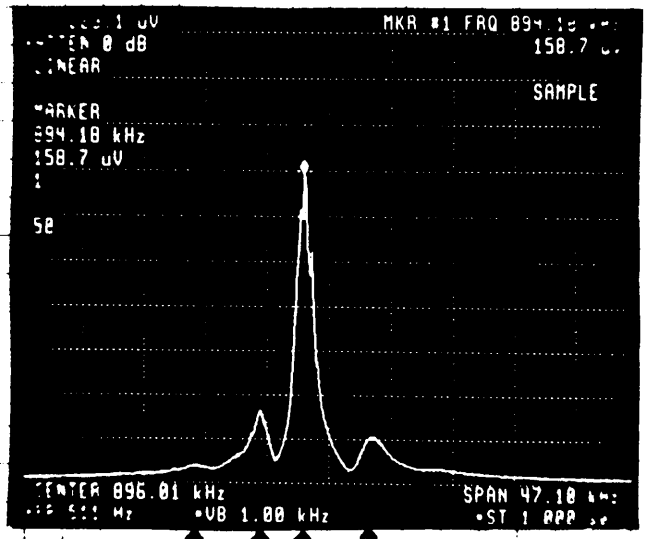

-2 -1 0 +1

$1.02\ 10^{10}\ e^+$

(b)

Modes N/h

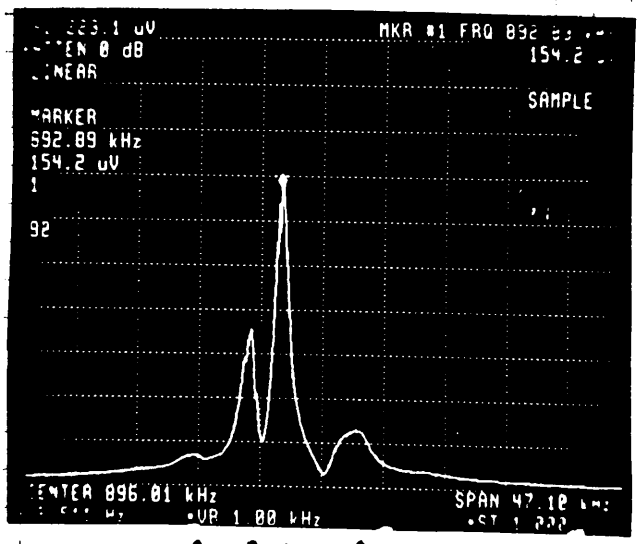

-2 -1 0 +1

$2.0\ 10^{10}\ e^+$

(c)

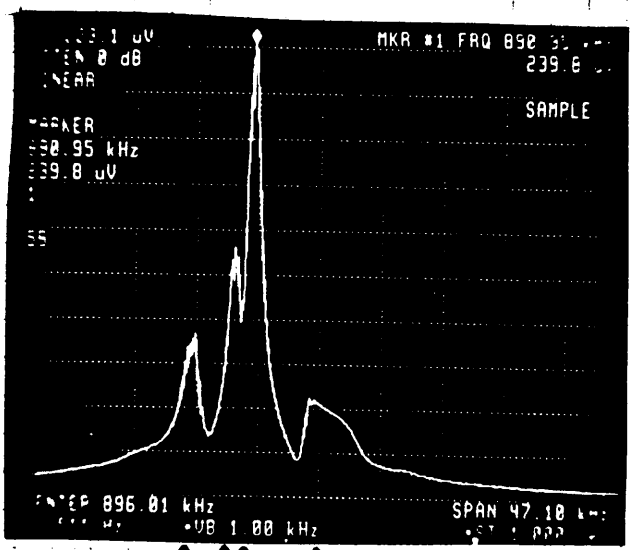

-2 -1 0 +1

$4.0\ 10^{10}\ e^+$

(d)

Modes N/h

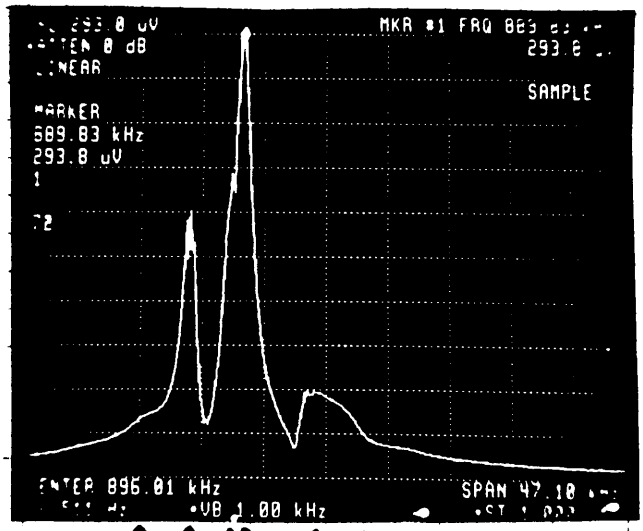

-3 -2 -1 0 +1

$5.5\ 10^{10}\ e^+$

(e)

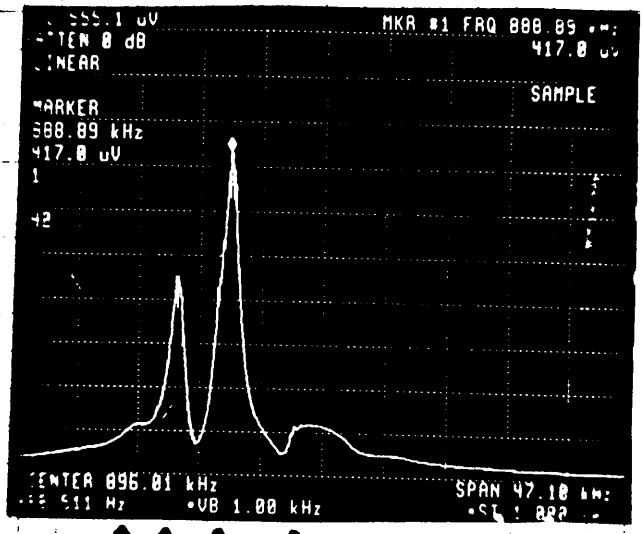

-3 -2 -1 0 +1

$7.0\ 10^{10}\ e^+$

(f)

Modes N/h

POSITRON SINGLE BUNCH VERTICAL MODE

fig 4

E = 500 MeV Q'_y = +2.0 V_{RF} = 45 kV

f_{y_0} = 864.8 kHz Q'_x = +0.1 F_{s_0} = 4.71 kHz

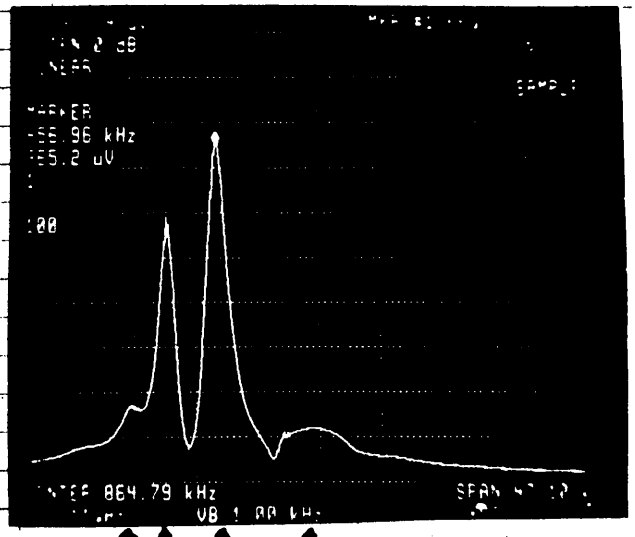

-3 -2 0/-1 +1

(g) 9. 10^{10} e+ N/k

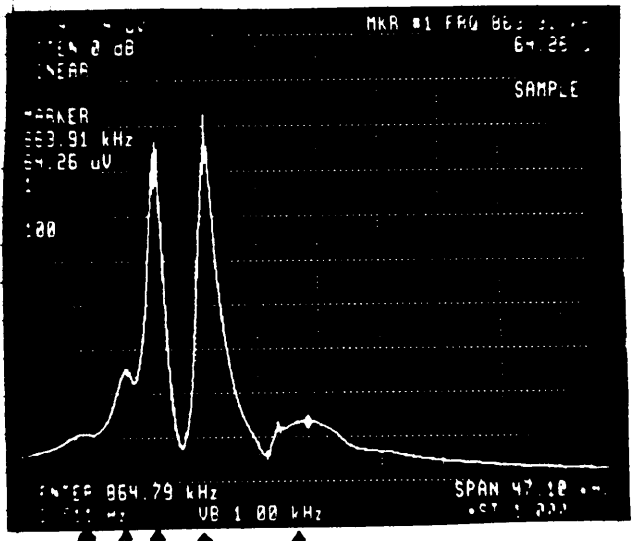

-4 -3 -2 0/-1 +1

Modes

10.8 10^{10} e+ (h)

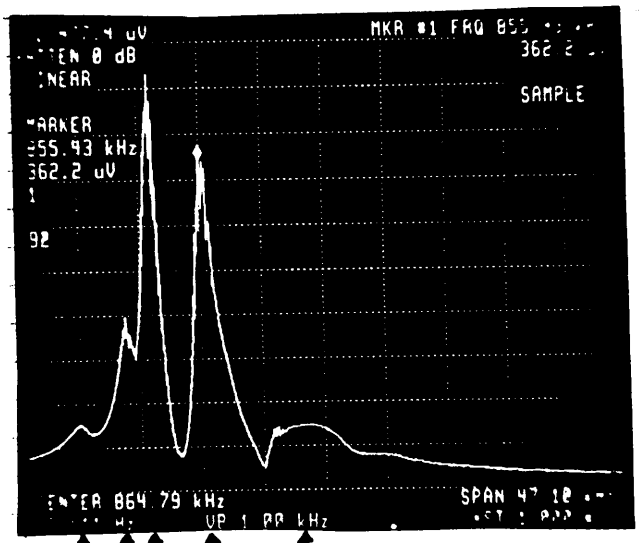

-4 -3 -2 0/-1 +1

(i) 12.5 10^{10} e+ N/k

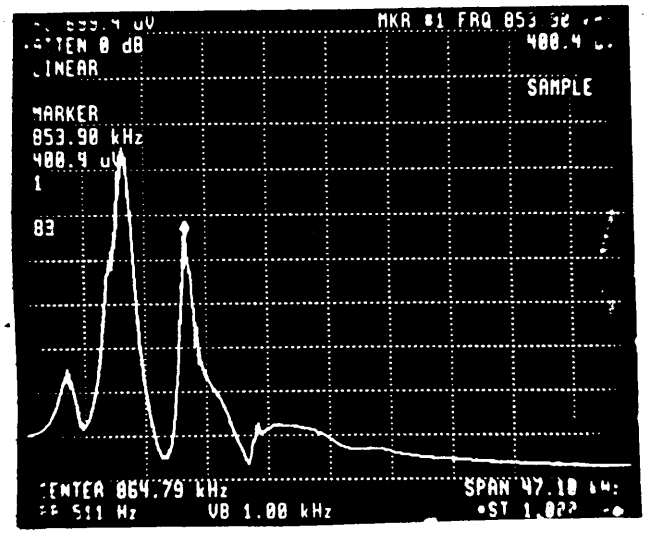

-4 -2/-3 0/-1 +1

Modes

17.5 10^{10} e+ (j)

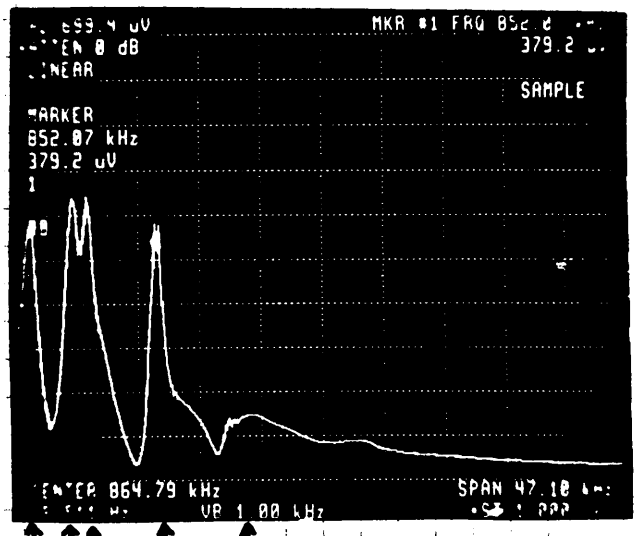

-4 -2 -3 0/-1 +1

(k) 24.0 10^{10} e+ N/k

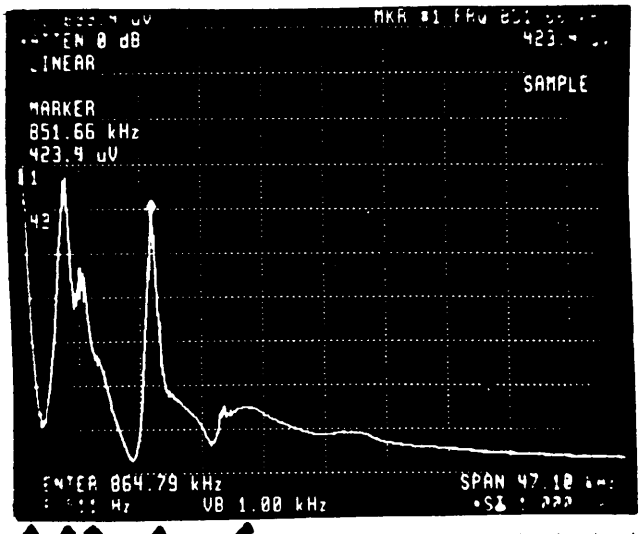

-4 -2 -3 0/-1 +1

Modes

28.0 10^{10} e+ (l)

Position Single Bunch Vertical Modes (July 87)

E = 500 MeV $Q'_y = +4.0$ $Q'_x = +0.1$ $V_{RF} = 15$ kV $F_s = 4.71$ kHz

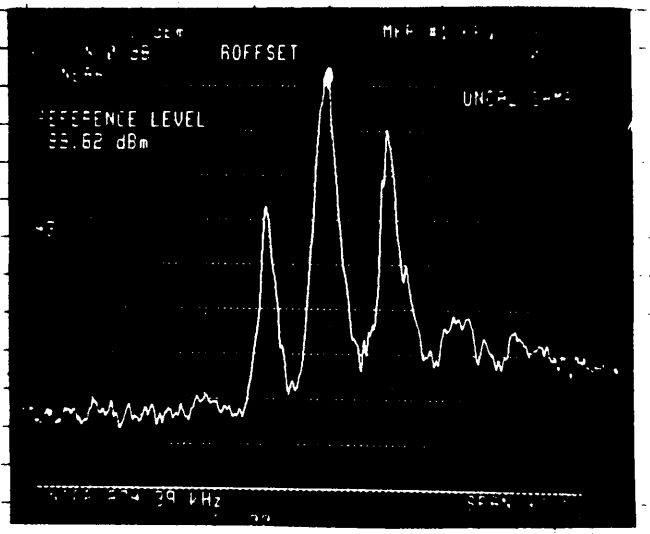

Modes -2 -1 0 +1 +2 +3

$N = 1.5 \times 10^9$ e+

(a)

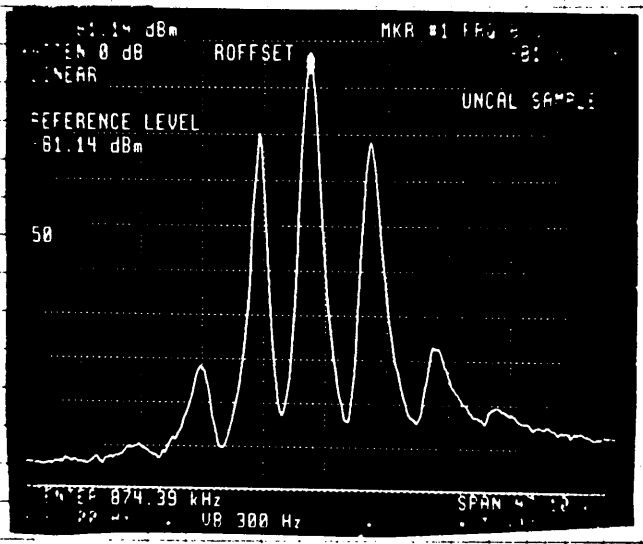

Modes -2 -1 0 +1 +2 +3

$N = 6.5 \times 10^9$ e+

(b)

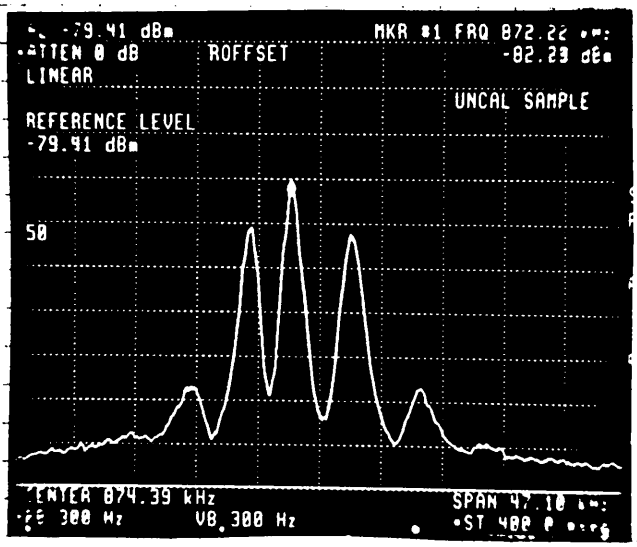

Modes -2 -1 0 +1 +2

$N = 1 \times 10^{10}$ e+

(c)

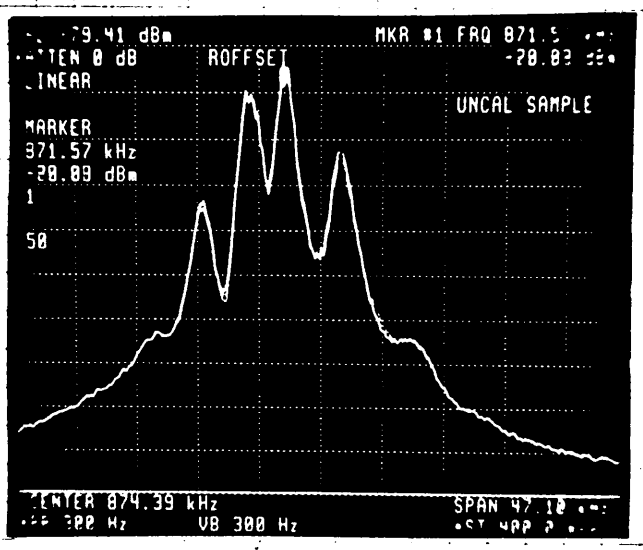

Modes -2 -1 0 +1 +2

$N = 2 \times 10^{10}$ e+

(d)

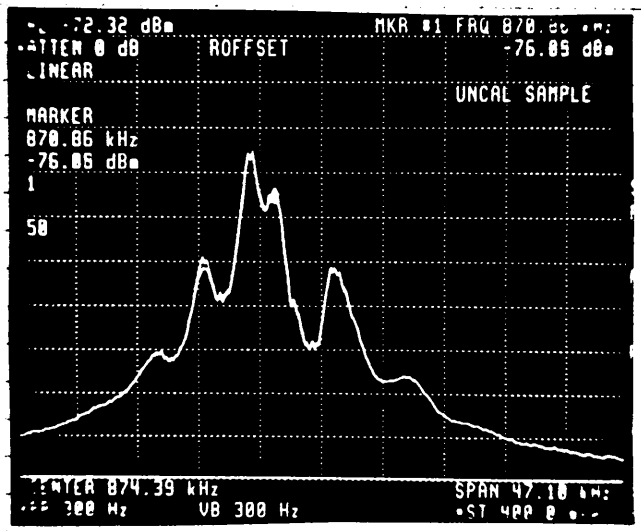

Modes -3 -2 -1 0 +1 +2

$N = 3 \times 10^{10}$ e+

(e)

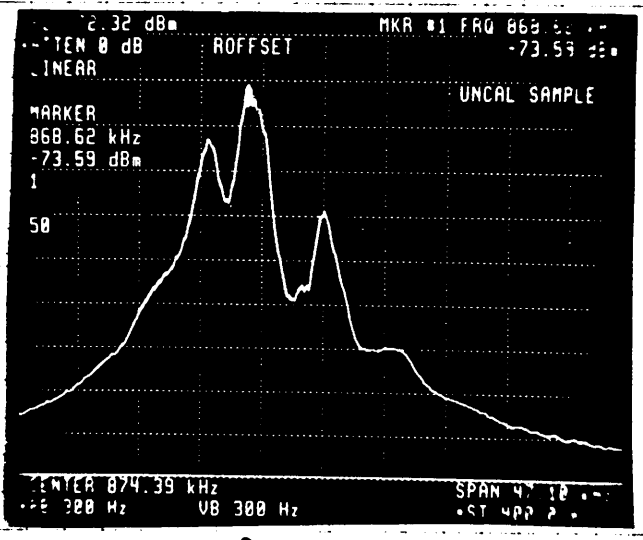

Modes -2 $\frac{0}{-1}$ +1 +2

$N = 4 \times 10^{10}$ e+

(f)

- fig 5 -

Position Single Bunch Vertical Modes (July 87)

E : 500 MeV $Q'_y = +4.0$ $V_{RF} = 45$ kV

$Q'_x \sim +0.1$ $F_s = 4.71$ kHz

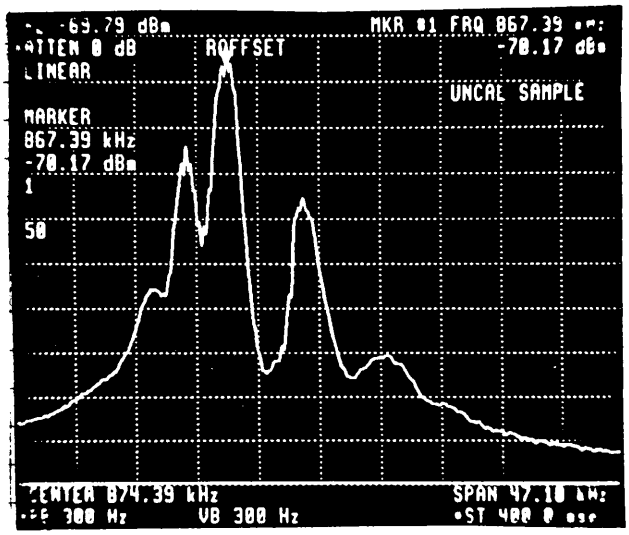

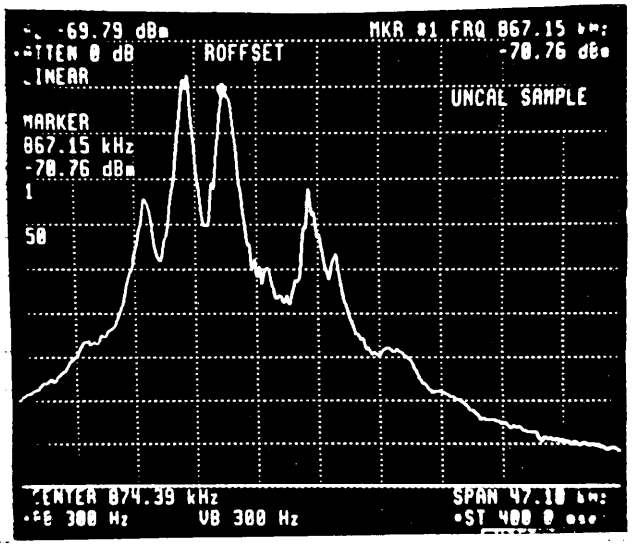

Modes -3 -2 -1 0 +1 +2

(g) $N = 5.10^{10}$ e+

Modes -3 -2 -1 0 +1 +2

(h) $N = 6 \times 10^{10}$ e+

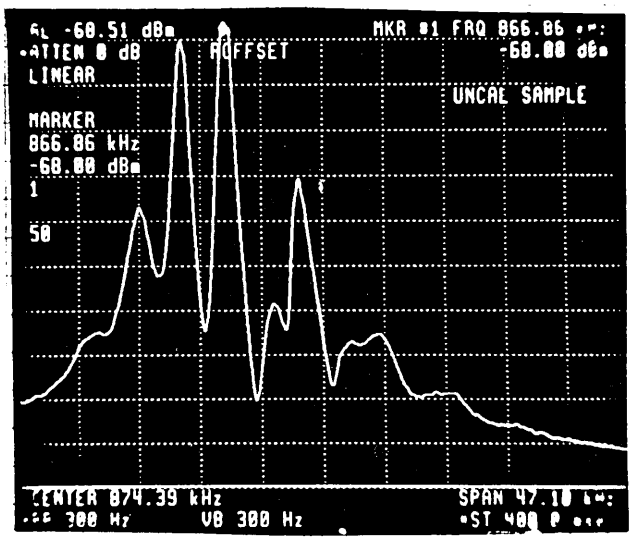

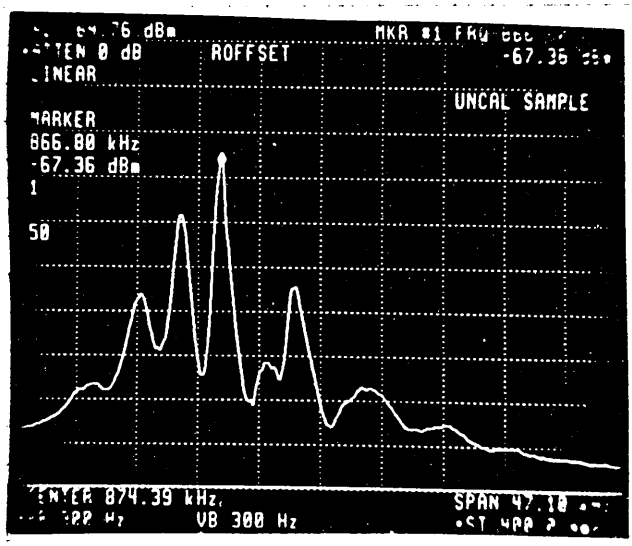

Modes -4 -3 -2 -1 0 +1 +2 +3

(i) $N = 7.10^{10}$ e+

Modes -4 -3 -2 -1 0 +1 +2 +3

(j) $N = 7.10^{10}$ e+

Position Single Bunch Vertical Modes (July 87)

- fig 6 -

E = 500 MeV $Q'_y = +2.0$ $Q'_x = +0.1$ V_{RF} = 20 kV f_s = 3.12 kHz

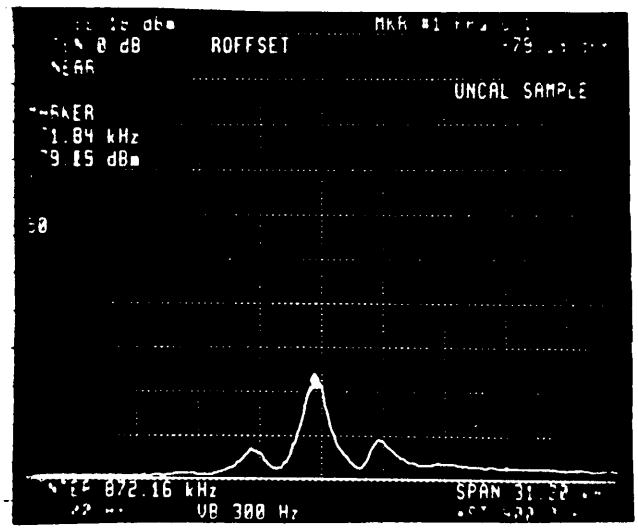

(a) Modes -1 0 +1
N = 1.5 10^9 e+

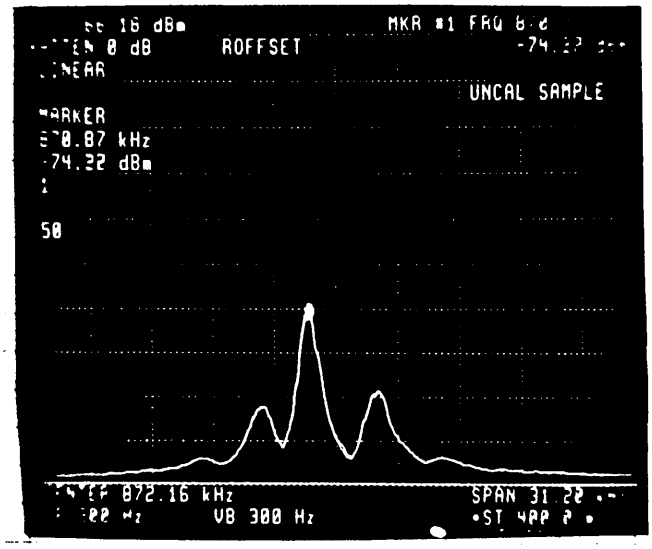

(b) Modes : -2 -1 0 +1 +2
N = 1×10^{10} e+

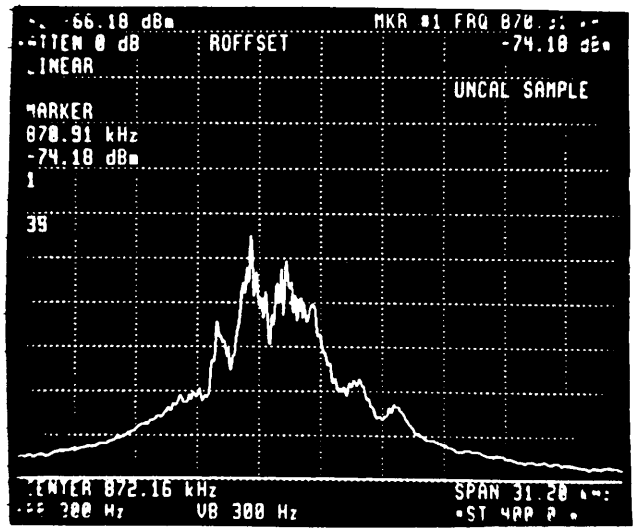

(c) Modes -2 -1 0 +1 +2 ?
N = 2.10^{10} e+

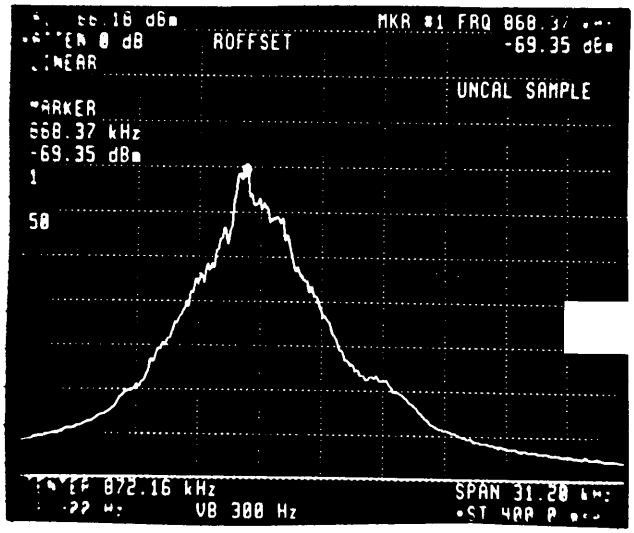

(d) Modes : ?
N = 3×10^{10} e+

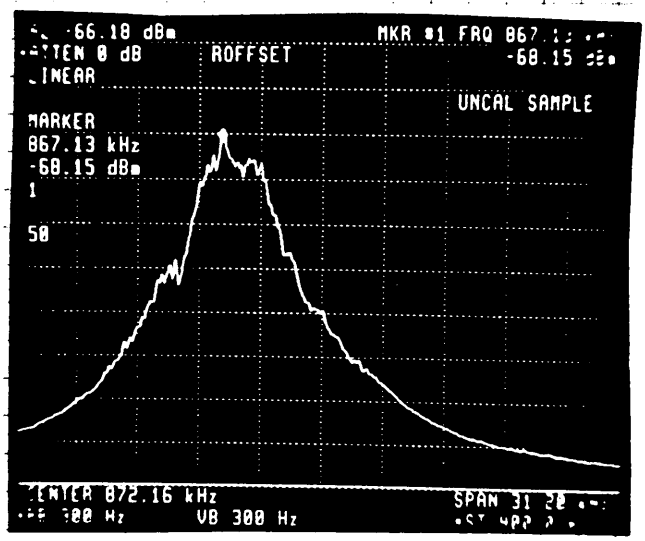

(e) N = 4×10^{10} e+

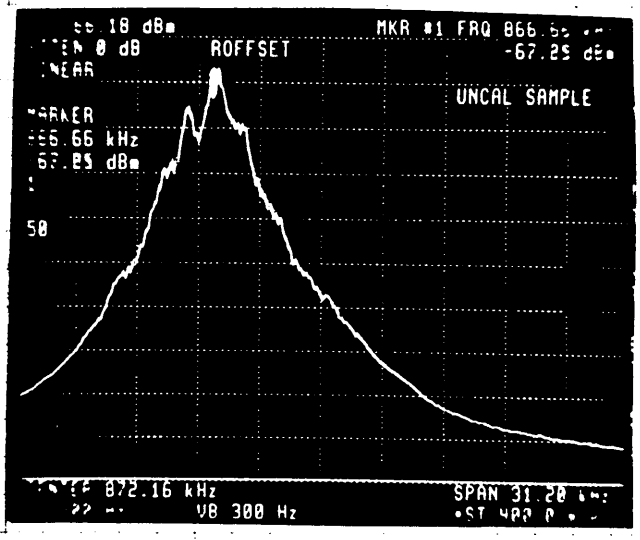

(f) N = 5.5×10^{10} e+

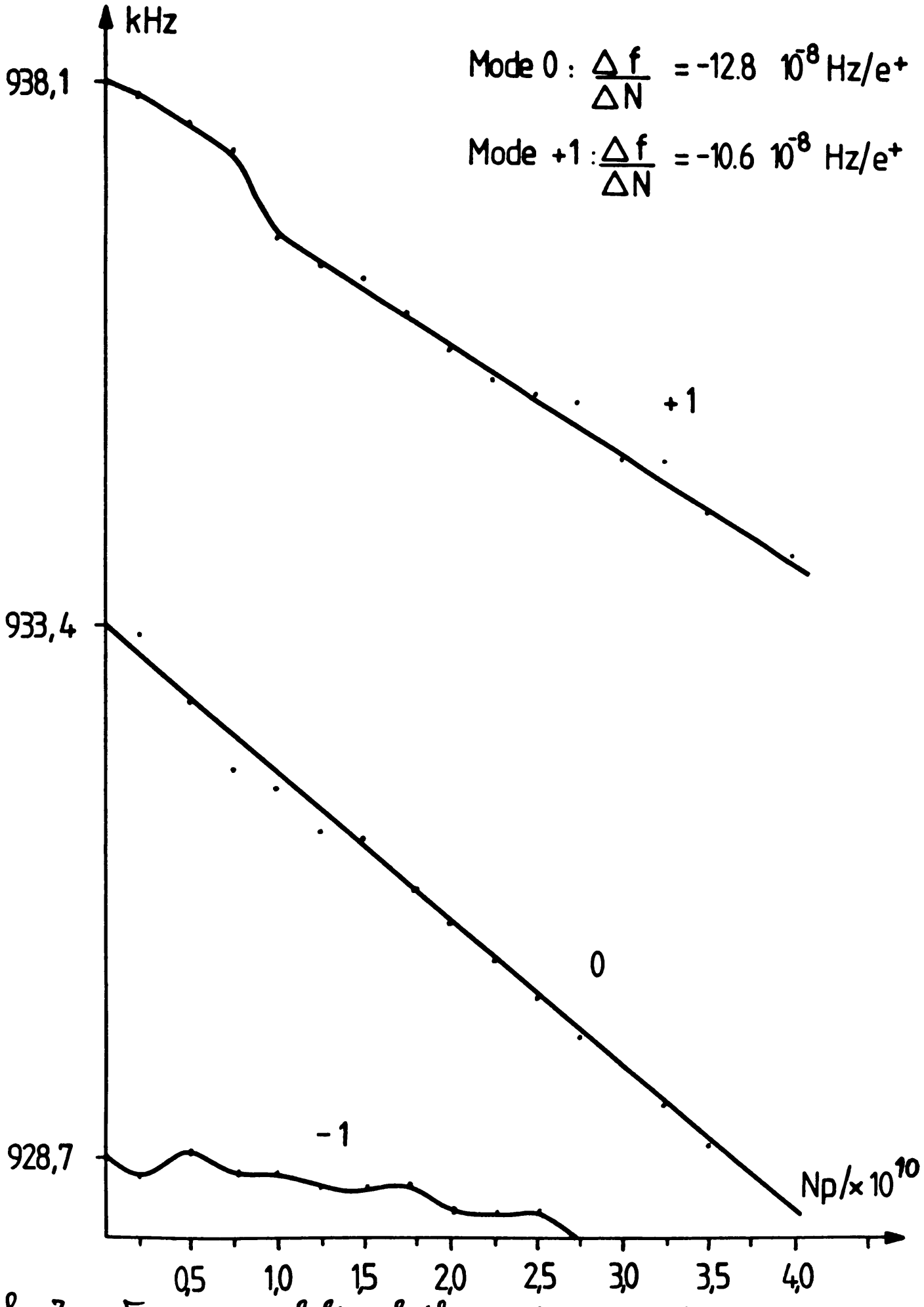

fig 7 : Frequency shift of the modes 0 and ± 1 in an exploratory measurement (Test 3 of table 1)

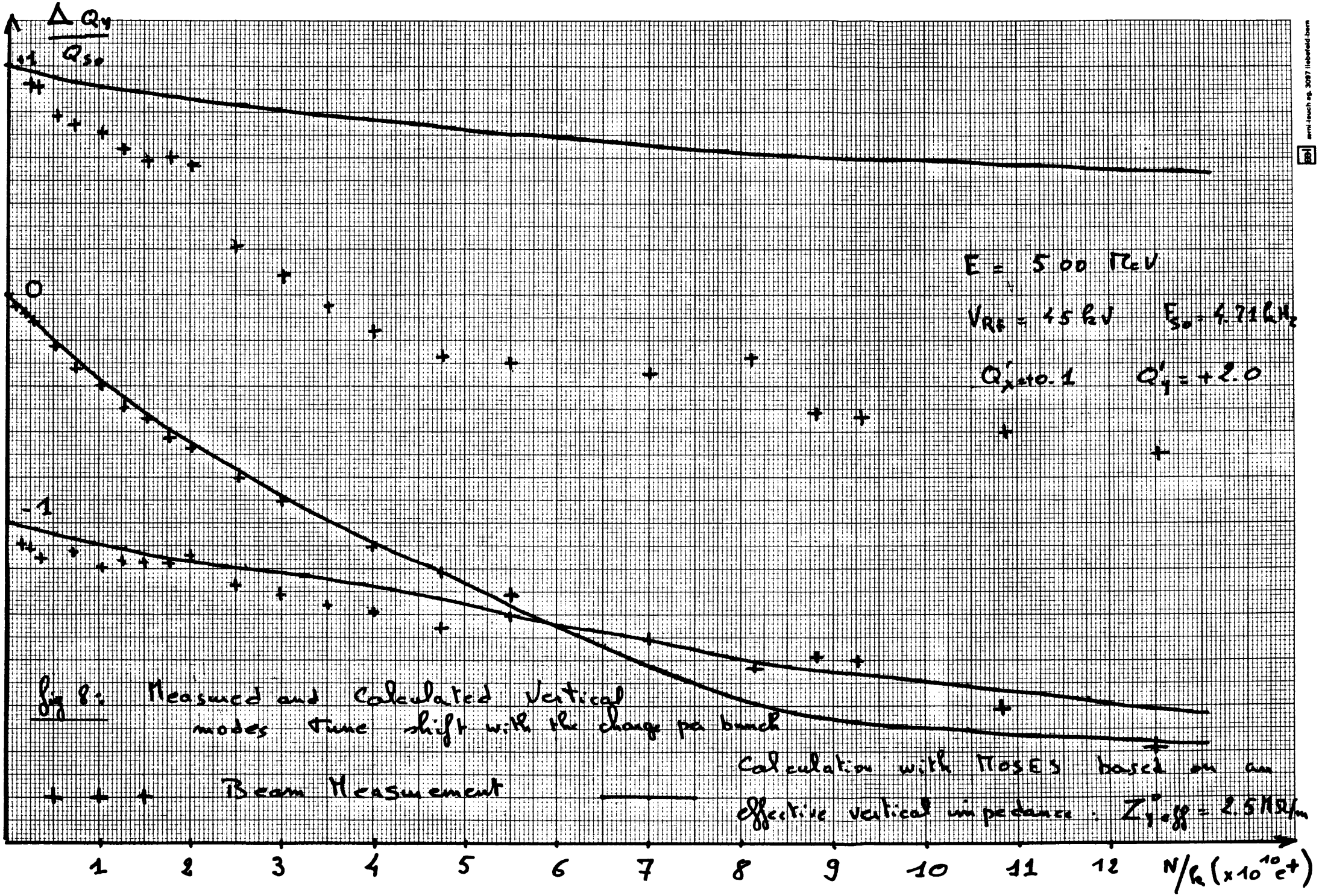

Fig 8: Measured and Calculated Vertical modes tune shift with the charge per bunch

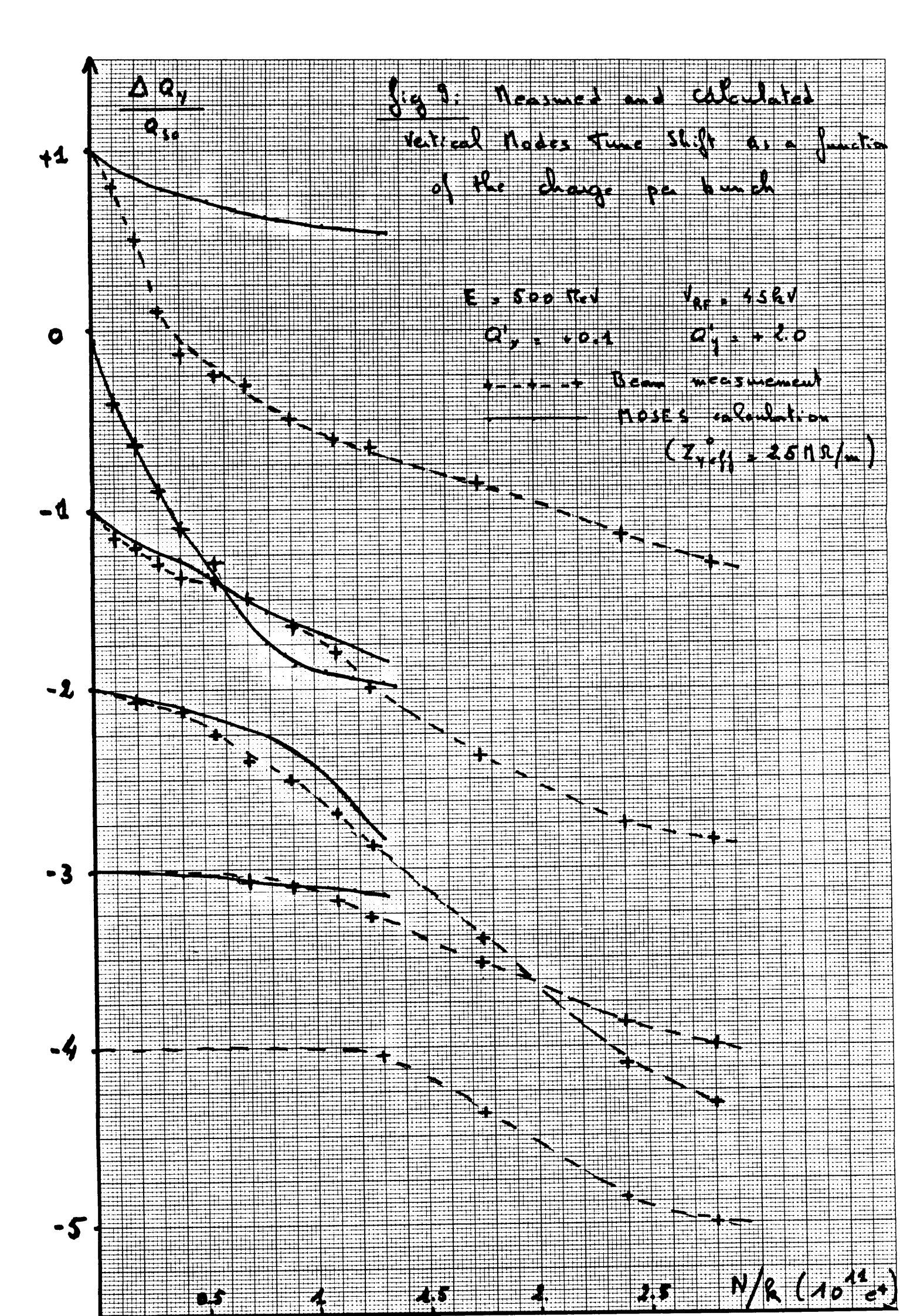

Fig 9: Measured and calculated Vertical Modes Tune Shift as a function of the charge per bunch

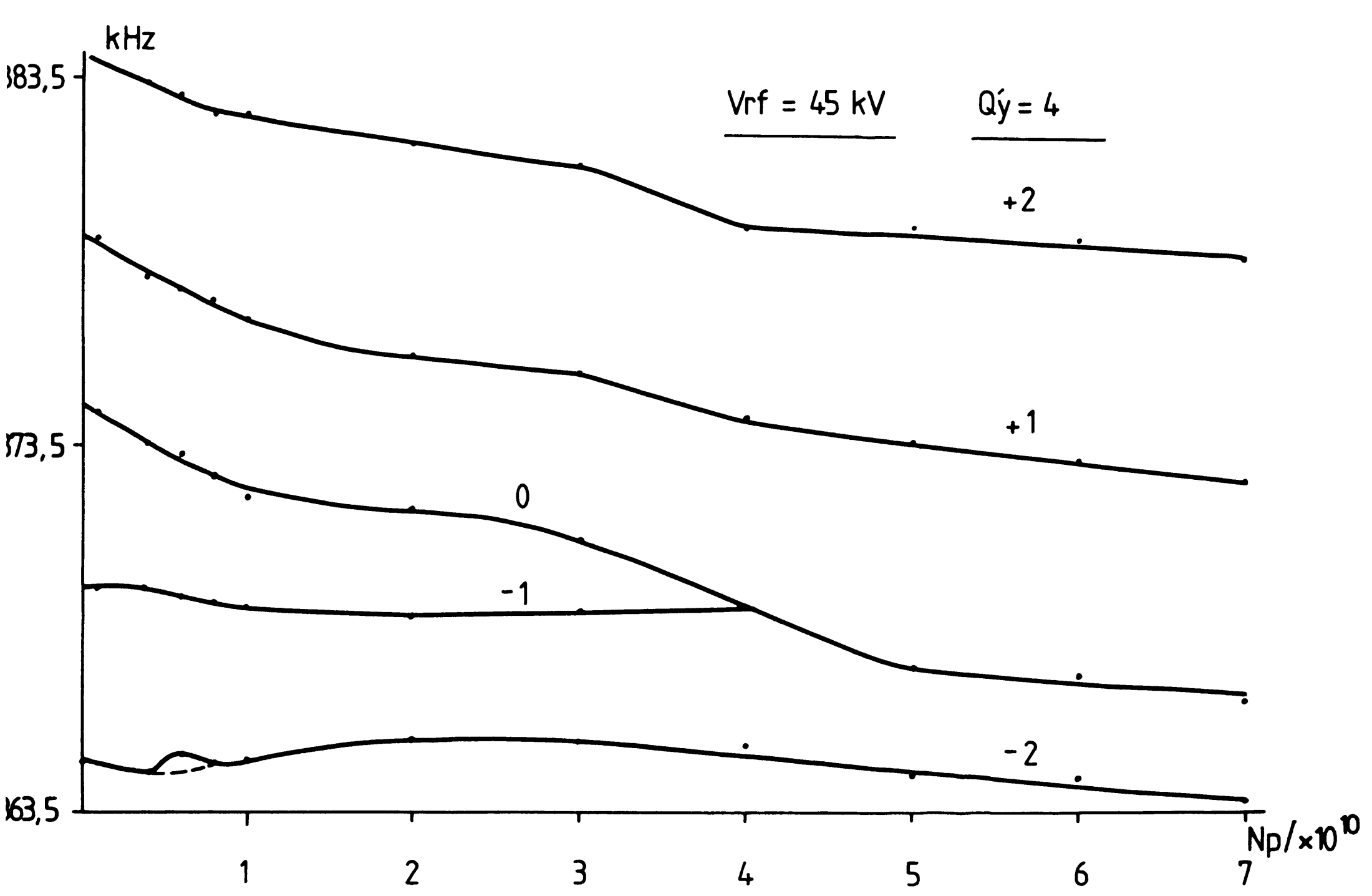

Fig 10 : Measured frequency shift of the vertical modes with a high chromaticity

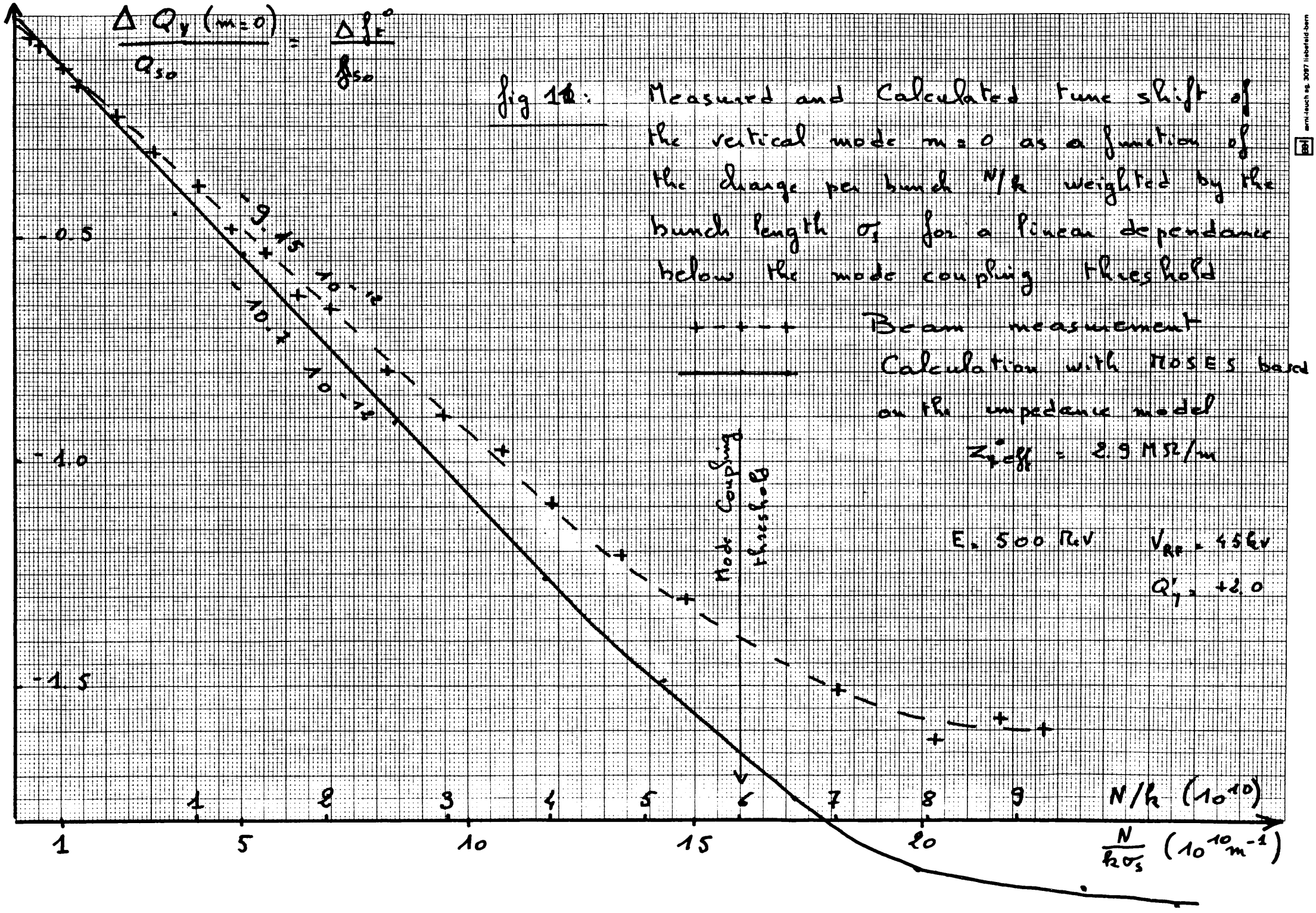

Fig 11: Measured and Calculated tune shift of the vertical mode m = 0 as a function of the charge per bunch N/k weighted by the bunch length σ_s for a linear dependance below the mode coupling threshold

+--+--+ Beam measurement

——— Calculation with MOSES based on the impedance model

$Z_{\perp}^{\circ}{}_{eff}$ = 2.9 MΩ/m

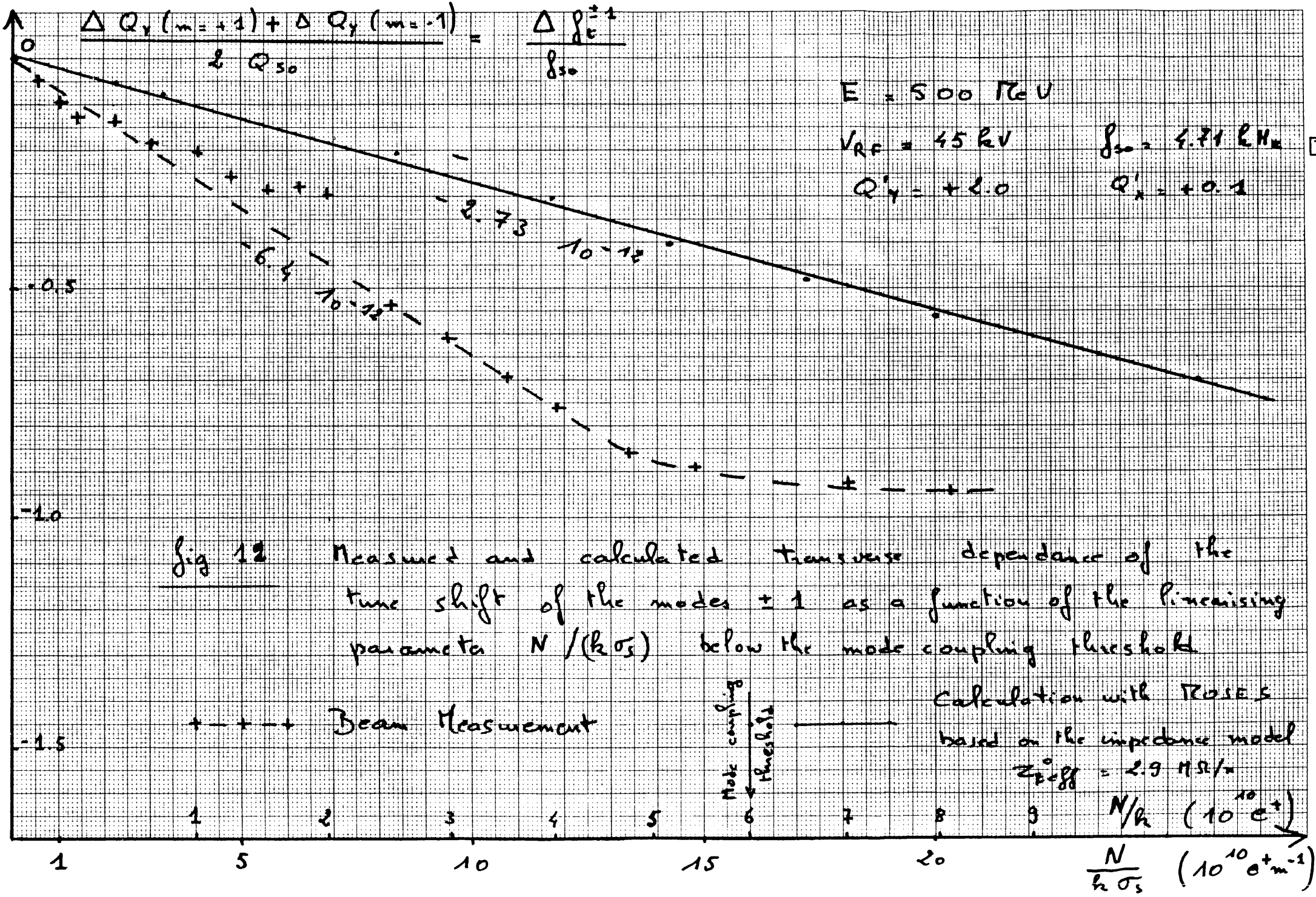

Fig 12 Measured and calculated transverse dependance of the tune shift of the modes ±1 as a function of the Pincensing parameter $N/(k\sigma_s)$ below the mode coupling threshold

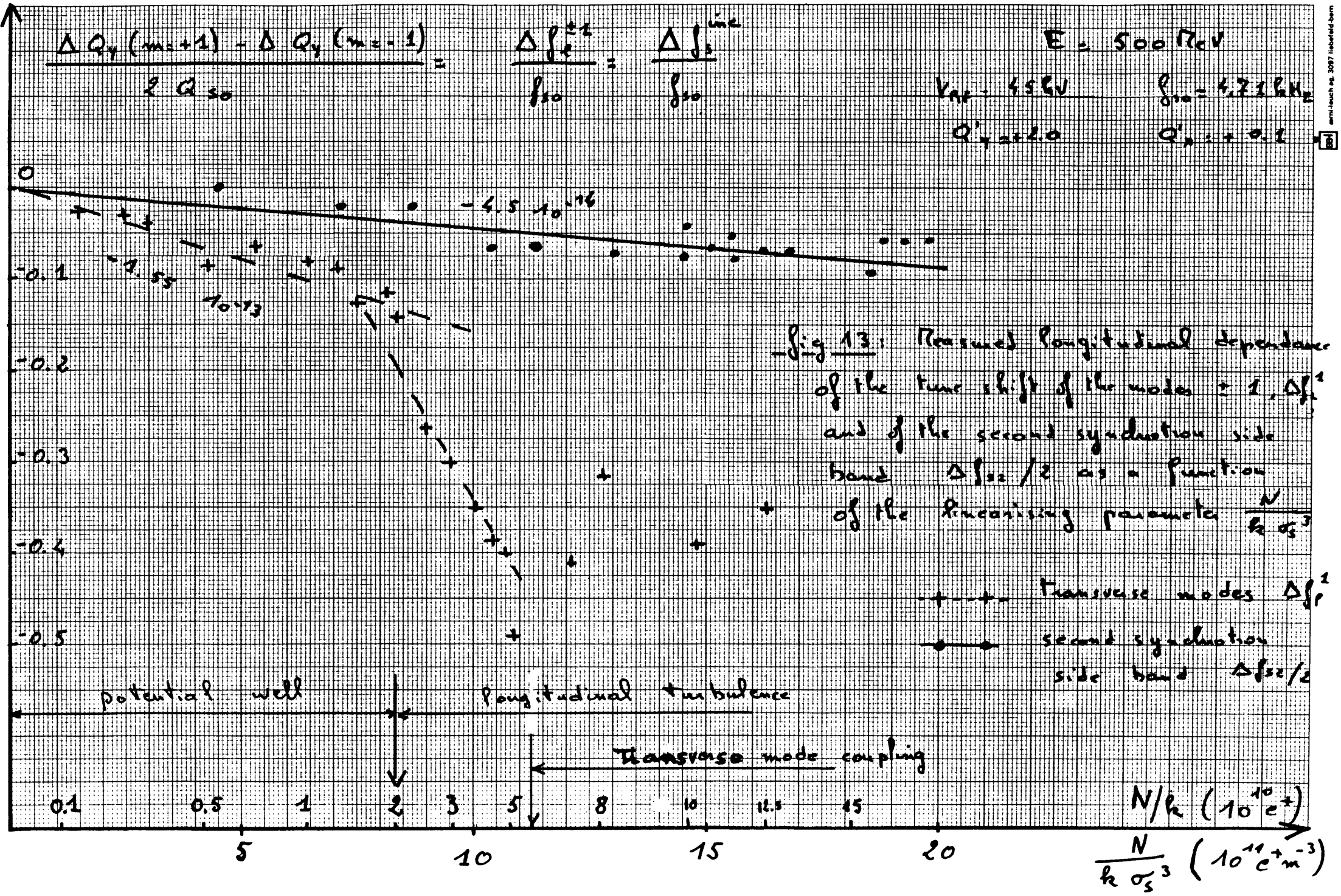

Fig 13: Measured longitudinal dependance of the tune shift of the modes ± 1, $\Delta f_s^{\pm 1}$ and of the second synchrotron side band $\Delta f_{sz}/2$ as a function of the bunching parameter $\frac{N}{k\sigma_s^3}$

Transverse modes $\Delta f_p^{\pm 1}$

second synchrotron side band $\Delta f_{sz}/2$

Fig 14 : Variation with current of the first and second synchrotron side band around the 20 th harmonic of the RF frequency

$E = 500$ MeV $\quad V_{RF} = 45$ kV $\quad f_s = 4.71$ kHz

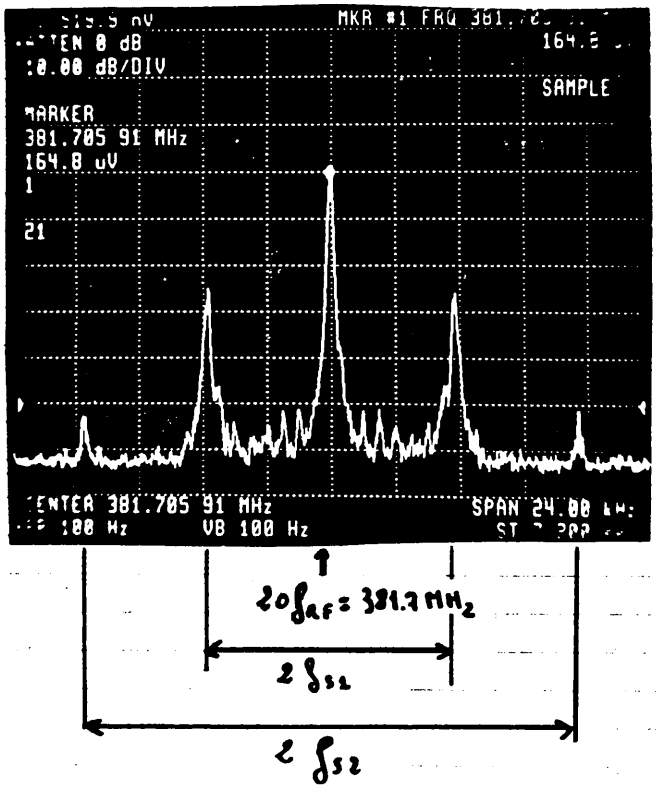

$N/k = 1.5\ 10^9\ e^+$

$f_{s1} = 4.71$ kHz

$f_{s2} = 9.36$ kHz

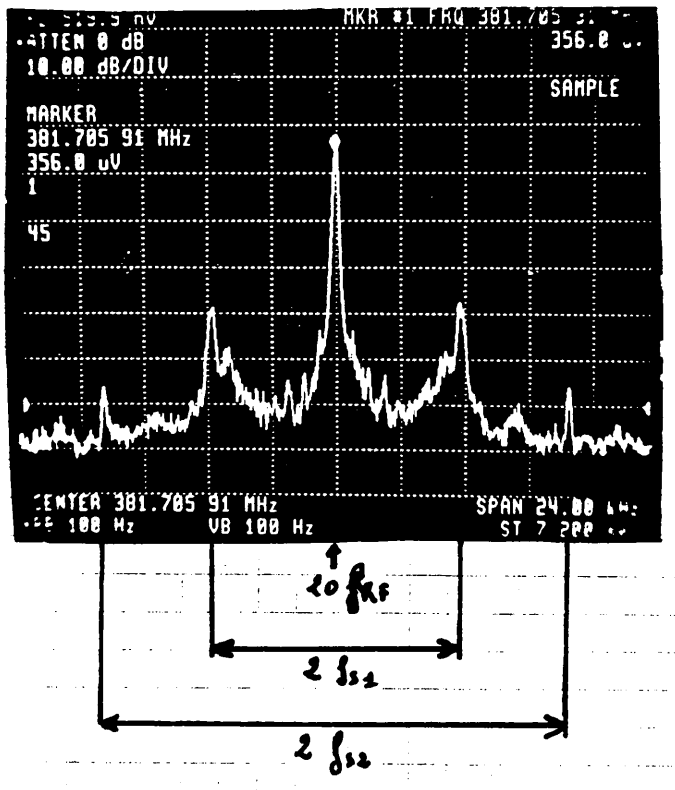

$N/k = 1.2\ 10^{11}\ e^+$

$f_{s1} = 4.71$ kHz

$f_{s2} = 8.78$ kHz